
This is the **published version** of the master thesis:

Nasarre Campo, Carles; García García, Joan J. , dir. Study of rectennas for RF Harvesting systems. 2020. 62 pag. (1170 Màster Universitari en Enginyeria de Telecomunicació / Telecommunication Engineering)

This version is available at <https://ddd.uab.cat/record/259445>

under the terms of the  license



**Universitat Autònoma
de Barcelona**

A Thesis for the
Master in Telecommunication Engineering

Study of rectennas for RF Harvesting systems

by
Carles Nasarre Campo

Supervisor: Joan J. García García
Department of Electronic Engineering

Escola d'Enginyeria
Universitat Autònoma de Barcelona (UAB)

January 2020



Els sotasignat, *Joan García*, Professor de l'Escola d'Enginyeria de la Universitat Autònoma de Barcelona (UAB).

FA CONSTAR:

Que el projecte presentat en aquesta memòria de Treball Fi de Màster ha estat realitzat sota la seva direcció per l'alumne *Carles Nasarre Campo*.

I, perquè consti a tots els efectes, signa el present certificat.

Bellaterra, 24 de Gener de 2020

Signatura:

INDEX

1	Introduction	1
1.1	Motivation	1
1.2	Objectives.....	2
2	RF energy harvesting system	3
2.1	State of the art [4].....	4
2.2	Precedent	5
3	Theory	7
3.1	Schottky diode.....	7
3.2	Rectenna.....	9
4	Simulation study.....	11
4.1	Analysis.....	14
4.2	Scalability.....	17
5	Implementation.....	19
5.1	Fabrication.....	19
5.2	Study in low frequency	21
5.3	Study in high frequency	24
6	Non-linearity in high frequency	33
6.1	Harmonic distortion [5]-[6].....	33
6.2	Resolution in high frequency	34
7	Implementation in the RF harvesting	41
8	Conclusions	45
9	References	47
10	Annex	49
10.1	Annex 1 - Paper PATMOS 2018 [6].....	49
10.2	Annex 2 - Datasheet of the Schottky diode SMS7630 [8]	52
10.3	Annex 3 - Datasheet of the SMD ceramic capacitor of 0.1 μ F [13].....	53
10.4	Annex 4 - Datasheet of the 2.4 GHz/ 5 GHz Wi-Fi antenna[14]	53

INDEX OF ILLUSTRATIONS

Figure 1. Number of related publications of RF Harvesting in the last 10 years. [2]	2
Figure 2. Architecture of an energy autonomous system.[3]	3
Figure 3. Evolution of the rectification capabilities of different diode technologies over the years.[4].....	5
Figure 4. Schematic circuit of the Harvesting system.	6
Figure 5. Comparison of characteristics of Schottky diode and a conventional diode.[7].....	8
Figure 6. Types of rectifiers a) Half wave rectifier and b) Full wave rectifier.	9
Figure 7. Study topologies a) Half wave rectifier, b) Voltage doubler, c) Full wave rectifier and d) Greinacher circuit.....	11
Figure 8. Forward bias current vs forward voltage simulated from the Schottky diode [8]	11
Figure 9. Schematic of a half wave circuit.....	12
Figure 10. Schematic of a full wave bridge rectifier or bridge rectifier.	12
Figure 11. Schematic of a half-wave voltage doubler.....	13
Figure 12. Schematic of a full wave series multiplier or Greinacher circuit.....	14
Figure 13. Comparison of the output voltages between study circuits in low frequency (1 kHz)	14
Figure 14. Comparison of the output voltages between study circuits in high frequency (100 MHz).	15
Figure 15. Representation of the voltage drop at the diode of the Half wave rectifier and Full wave rectifier.....	16
Figure 16. Representation of the output voltage of the multiplier circuits: Voltage doubler and Greinacher circuit.	17
Figure 17. Representation of a) the scaled Voltage doubler circuit and b) the output voltage as a function of time.	18
Figure 18. Instrumentation used for the fabrication of the circuits: a Leica microscope and a JBC solder station.	19
Figure 19. Impedance vs frequency response characteristic for a capacitor.[11].....	20
Figure 20. Implementation of a) the Half wave rectifier, b) the Voltage doubler circuit, c) the Full wave rectifier and d) the Greinacher circuit (see the schematics circuit in Figure 7).....	21
Figure 21. Instrumentation used for low frequency characterization: a digital oscilloscope.	22
Figure 22. Results obtained in the oscilloscope for an input of 500 mV at 1 kHz in a) the Half wave rectifier, b) the Voltage doubler, c) the Full wave rectifier and d) the Greinacher circuit. 23	
Figure 23. Results obtained in the oscilloscope for an input of 50 mV at 1 kHz in a) the Half wave rectifier, b) the Voltage doubler, c) the Full wave rectifier and d) the Greinacher circuit. 24	
Figure 24: Instrumentation used for high frequency circuit characterization: a Multimeter, a Network analyzer and a Spectrum analyzer.	25
Figure 25. Calibration at 0 dBm of a) the Network analyzer with b) the Spectrum analyzer.	26
Figure 26. Representation of a) the impedance, b) the input voltage and c) the output voltage of the Full wave rectifier respect to the power introduced.	28
Figure 27. Representation of a) the impedance, b) the input voltage and c) the output voltage of the Voltage doubler circuit respect to the power introduced.....	29
Figure 28. Representation of a) the impedance, b) the input voltage and c) the output voltage of the Greinacher circuit respect to the power introduced.....	30
Figure 29. Small-signal model of a diode in high frequency.[5].....	33
Figure 30. Example of harmonic distortion seen in the frequency domain of the output and the distortion components.[12].....	33

Figure 31. a) Delta sent in $f_0=2.4\text{GHz}$. b) Decomposition of the delta at the output of the rectifier.[5]-[6]	34
Figure 32. Implementation of a) the Half wave rectifier, b) the voltage doubler circuit, c) the Full wave rectifier and d) the Greinacher circuit, modified by adding a parallel capacitor at the output of each circuit.....	35
Figure 33. Results obtained in the oscilloscope for an input of 500 mV at 1kHz of a) the Half wave rectifier, b) the Voltage doubler circuit, c) the Full wave rectifier and d) the Greinacher circuit, modified by adding a parallel capacitor at the output of each circuit.	35
Figure 34. Results obtained in the oscilloscope for an input of 50 mV at 1kHz of a) the Half wave rectifier, b) the Voltage doubler circuit, c) the Full wave rectifier and d) the Greinacher circuit, modified by adding a parallel capacitor at the output of each circuit.	36
Figure 35. Representation of a) the impedance, b) the input voltage and c) the output voltage of the Full wave rectifier respect to the power introduced, modified by adding a parallel capacitor at the output of each circuit.	37
Figure 36. Representation of a) the impedance, b) the input voltage and c) the output voltage of the Voltage doubler circuit respect to the power introduced, modified by adding a parallel capacitor at the output of each circuit.	38
Figure 37. Representation of a) the impedance, b) the input voltage and c) the output voltage of the Greinacher circuit respect to the power introduced, modified by adding a parallel capacitor at the output of each circuit.	39
Figure 38. Frequency response of the antenna for a frequency range of 6 GHz obtained with the measurement environment described.	41
Figure 39. Monitoring of the Half wave circuit accumulated load with the antenna.	42
Figure 40. Monitoring of the Full wave rectifier accumulated load with the antenna.	43
Figure 41. Monitoring of the Voltage doubler circuit accumulated load with the antenna.....	43
Figure 42. Monitoring of the Greinacher circuit accumulated load with the antenna.....	44
Figure 43. Spice parameters of the Schottky diode SMS7630.....	52
Figure 44. a) Typical detector characteristics at 1.8 GHz and b) Forward voltage vs forward bias current for the Schottky diode.....	52
Figure 45. Variation of impedance with chip size vs frequency for 0,1 μF	53
Figure 46. Electric specifications of the Wi-Fi antenna.....	53

INDEX OF TABLES

Table 1. The power consumption of typical wireless electronic devices.[1]	1
Table 2.Comparison between Schottky diode and conventional diode (p-n junction diode).[7] ..	8

1 INTRODUCTION

1.1 MOTIVATION

In the near future, a *boom* of the number devices connected to the Internet is foreseen, which will impose tremendous challenge, both, in terms of spectrum and power supply. On the one hand, new communication protocols and wider bandwidths will be developed to manage this huge number of heterogeneous user. On the other hand, according to the emerging Internet of Things (IoT) paradigm, electronic devices will be deployed almost everywhere. The next generation of sensor and circuits will be literally embedded in items, so their maintenance will be difficult to reach or even to locate. This means that the battery replacement will be difficult or even impractical, so, in most of the cases, battery-less devices will be the only option left. This lack of power supplies or batteries can be covered by energy harvesting. This method implies recovering or reusing the wasted energy (in terms of power of thermal losses, vibrations, etc.) of already implemented systems. Bearing in mind the typical power recovering that an energy harvester can provide, consumptions of several devices such as mentioned in Table 1 can be covered easily.

Power	1 μ W	10 μ W	100 μ W	1 mW
Device	32 kHz Quartz oscillator	Watch, Calculator, Passive RFID	Hearing Aid, Temp. sensor	Active RFID, Miniature FM receiver

Table 1. The power consumption of typical wireless electronic devices.[1]

In the very last decade, the number of investigation that target the idea of achieving battery-less, energy scavenging devices has raised enormously due to their need and the advantages they can provide.

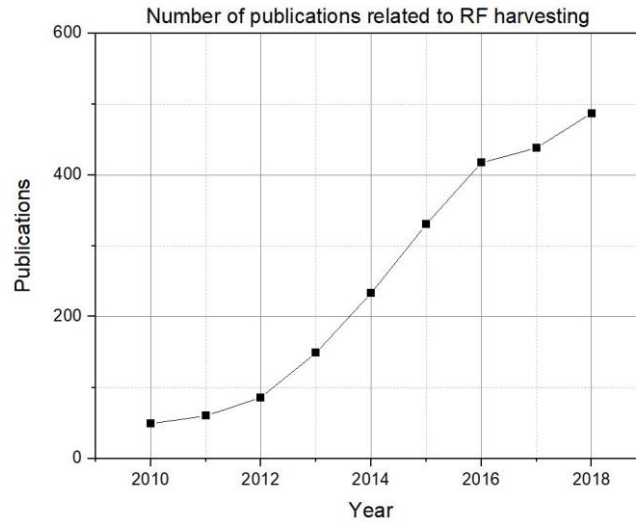


Figure 1. Number of related publications of RF Harvesting in the last 10 years. [2]

1.2 OBJECTIVES

The target of this project is to implement and characterize the rectifier circuits based on the publication of "A multi-band stacked RF energy harvester with an RF to DC efficiency of up to 84%" [1] to provide the required energy at the input of an energy harvester.

The project aims to demonstrate that it is possible to take advantage of energy gathering for a wide frequency band and achieve greater efficiency. To this end, the simulation of these circuits, in high and low frequency, and their subsequent implementation with experimental measures are performed. It is also to be observed if it is possible to improve the current circuits by scaling the circuits, in other words, combining their architectures to achieve greater potential at the output.

2 RF ENERGY HARVESTING SYSTEM

An Energy Autonomous System is an electronic system that has been designed to operate as long as possible providing, elaborating and storing information without being connected to a power grid. The systems could operate in external natural or industrial environments.

Nowadays this concept references the systems with the ability to operate with no more than a few μW of power within less than some cubic centimeters. Examples of such systems are devices operating at ultra-low power (as wireless sensor networks). It could be roughly divided into three parts:

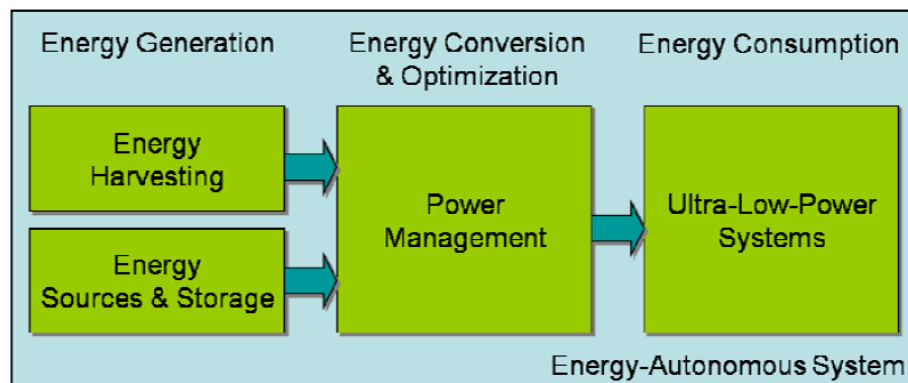


Figure 2. Architecture of an energy autonomous system.[3]

Energy Generation:

- **Energy Harvesting:** Takes into account any device or system that could harvest energy from correlated or uncorrelated sources of energy. It can be classified by the type of energy used: temperature, light radiation, electromagnetic fields, kinetic energy, etc.
- **Energy Sources:** any kind of energy storage element that could be used to accumulate energy from the harvester and provide it to the system whenever the energy is insufficient. Typically energy sources consist of electro- chemical elements such as batteries, fuel cells or electrical storage systems such as capacitors.

Energy Conversion and Optimization:

This refers to the exchange of any energy conversion within the system and there are two considerations to take into account: First, any source for the harvesting energy should be converted with respect to the existing sources. Second, the energy used by the device should be ideally equal or even less than what gained by the process itself.

Energy Consumption:

This section refers to the device's use of energy. This is relevant to the efficiency of the energy harvest, since the more the process is optimized, the more energy can be harvested.

Energy harvesting or scavenging is the conversion of ambient energy into electrical energy, by means of a specific transduction principle. Vibration, heat or solar energy are the main sources of ambient energy. In a strict definition, harvesting makes use of ambient energy which is not released on purpose and otherwise would be lost. An example of this case is the conversion of RF energy, which can be done in two ways.

- Take advantage of the existing electromagnetic radiations (e.g. GSM, FM, WiFi). Nonetheless, the energy density collected by this method is low (usually $\mu\text{W}/\text{cm}^2$).
- Emit an electromagnetic signal at a specific wavelength to power a device. Although the maximum power allowed to be transmitted into the environment is typically around 100mW.

2.1 STATE OF THE ART [4]

The harvested RF energy may be capable of providing input power on the order of tens of micro-watts or less. At this power level, RF to DC rectification is quite inefficient. But the problem is that the key element of the RF to DC converter, a non-linear device, is so influenced by the input power that all RF circuits are designed accordingly.

As device technologies advance, it is increasingly possible to operate with less power. However, harvesters could not because it is limited by the inherent physical and electrical properties of the rectifier devices used in the design of the harvesters for RF to DC power conversion.

In 1875 it was shown that there was a deviation from Ohm's law that led to the functional definition of the diode. This led to the creation of diodes and transistors. Nowadays, there are four main diode technologies, which compete to offer the highest deviation, i.e. non-linearity of current and voltage, which is responsible for the conversion of RF to DC power. The most crucial parameter to evaluate how successfully the diodes rectify is the short circuit current responsivity. This parameter is a direct function of the characteristic curvature $I(V)$, which relates the short circuit current obtained by the rectification and the voltage absorbed by the PN junction resistance.

Figure 3 below shows the trends in technological developments with respect to rectifiers.

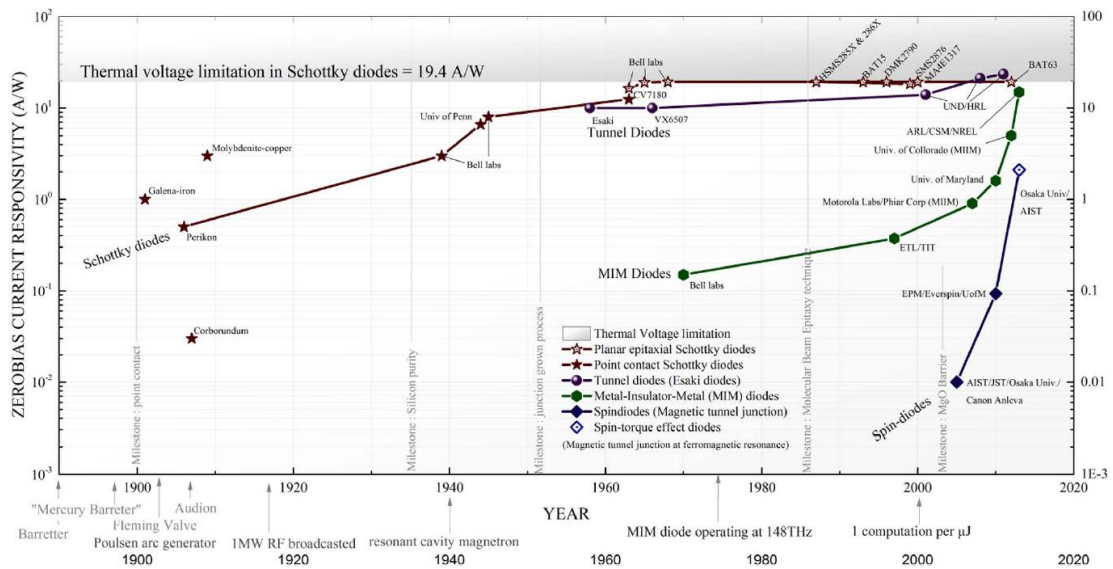


Figure 3. Evolution of the rectification capabilities of different diode technologies over the years.[4]

The most efficient way to deviate from Ohm's law is to limit the flow of electrons by using a potential barrier. Depending on the structural topology, the electron will probably move through the barrier by a thermal activation (e.g. Schottky's diode) or tunnel the barrier (e.g. tunnel diode, metal-insulator-metal (MIM) diode, spindiode) by a physical effect.

2.2 PRECEDENT

As mentioned above, the number of investigations that target the idea of achieving battery-less, energy scavenging devices has raised enormously due to their need and the advantages they can provide. Within the research group, various works related to the topic have been developed.

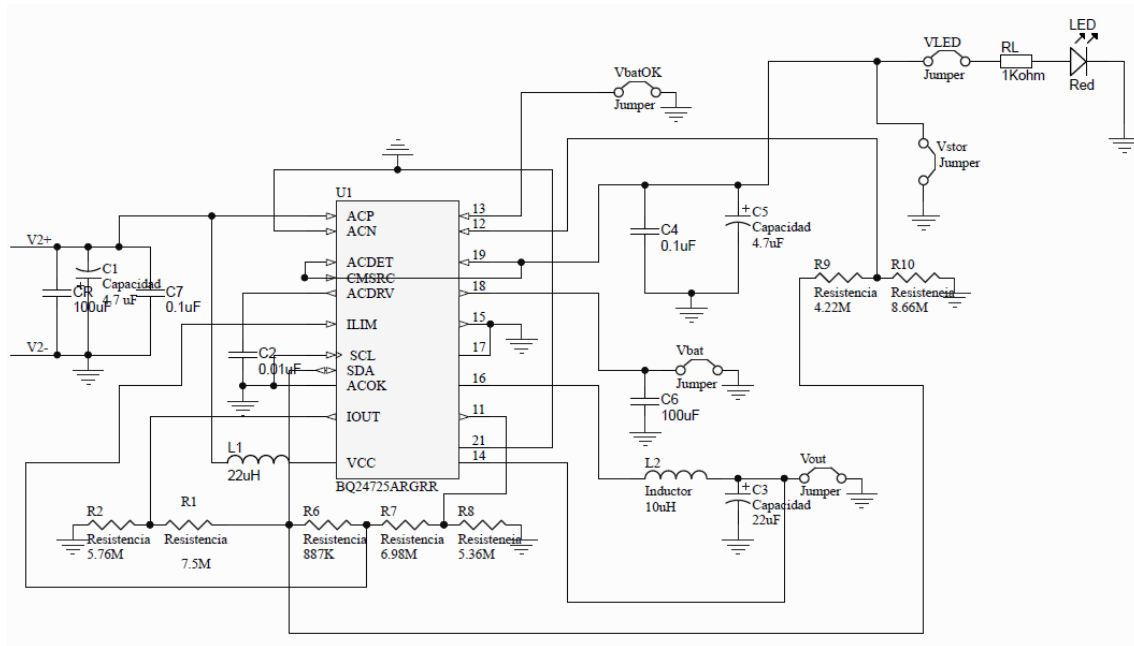


Figure 4. Schematic circuit of the Harvesting system.

GAEMI group has been working previously with harvesting devices, the schematic shown in Figure 4 has been fabricated, assembled and tested. In the rectification of the signal captured by an antenna, the option of full wave rectification was chosen, using the configuration of a diode bridge to take advantage of the maximum signal captured [5].

An alternative to impedance matching has been studied, in the context of power transfer, using resonant cavities to improve broadband energy collection and obtaining enough load to excite the energy management stage (see annex 10.1). [6]

3 THEORY

3.1 SCHOTTKY DIODE

At low frequencies the conventional diode can be easily turn off by changing its bias from forward to reverse. But at very high frequencies conventional diode shows a tendency to store the charge and there is noticeable current in reverse half cycle. During forward biased it is not possible for all the carriers in depletion region to recombine. Some carriers exist in depletion region which are not recombined. Now, if the diode is suddenly reverse biased the carriers existing in depletion region can flow in the reverse direction for some time. But for large life time of these carriers, longer is the flow of the current in reverse half cycle. Hence there is a limitation on the frequency range for which a conventional diode can be used.

The time taken by a diode to turn off from its forward biased state is called reverse recovery time. For frequencies up to 10 MHz it is very small but above 10 MHz it is large and puts a limit on the use of conventional diode in such high frequency applications.

The diodes which are specially manufactured to solve this problem of fast switching are called Schottky diodes. These diode are also called Schottky barrier diodes, surface barrier diodes or hot carrier diodes. Its construction is different than the conventional p-n junction diode.

Due to its construction, Schottky diode cannot store the charge, which allows it to switch off faster than a conventional diode. It can be easily switched off for the frequencies above 300 MHz. The barrier at the junction for a Schottky diode is less than that of normal p-n junction diode, in both forward and reverse bias region. The barrier potential and breakdown voltage in forward bias and reverse bias region respectively are also less than p-n junction diode. The barrier potential of Schottky diode is 0.25V as compared to 0.7 V for normal diode. The Figure 5 shows the comparison of characteristics of Schottky diode and a conventional p-n junction diode

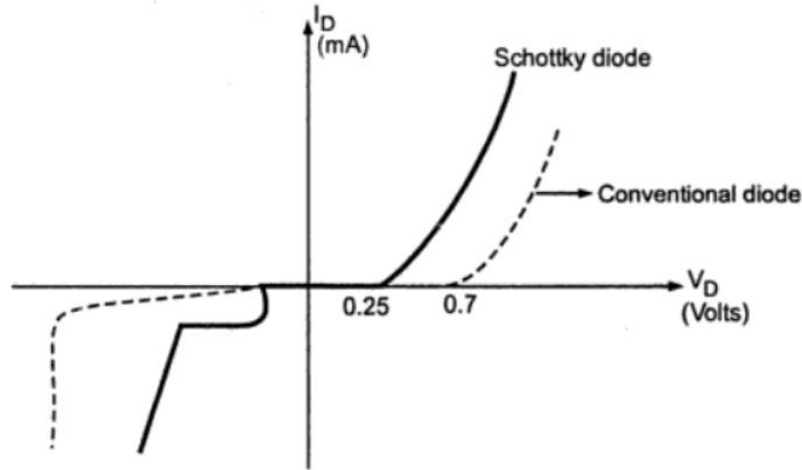


Figure 5. Comparison of characteristics of Schottky diode and a conventional diode.[7]

Briefly, the following differences between a conventional diode and a Schottky diode can be seen in Table 2. These characteristics of the Schottky diode make it an ideal diode for high frequencies and harvester circuits.

Parameter	p-n junction diode	Schottky diode
Junction	Semiconductor to semiconductor	Semiconductor to metal
Carriers	Minority and majority	Only majority
Reverse recovery time	More	Less
Barrier potential ¹	More about 0.7V	Less about 0.25V
Breakdown voltage	More	Less
Switching speed	Less	High
PIV ² rating	More	Less
Frequency range	Up to 10 Mhz	Very high more than 300 MHz
Applications	Mainly rectifiers and low frequency devices	High frequency devices, digital computers, radar systems, Schottky TTL logics, mixers, etc.

Table 2. Comparison between Schottky diode and conventional diode (p-n junction diode).[7]

¹ **Barrier potential (V_{γ}):** minimum voltage required to start current in P-N junction of semiconductors. It is the voltage to start current through a joint of two dissimilar materials. In diodes the barrier potential varies from 0.3 V to 0.7 V depending upon the semiconductor materials.

² **PIV:** Peak Inverse Voltage

3.2 RECTENNA

A rectenna is a rectifying antenna, a special type of receiving antenna that is used for converting electromagnetic energy into direct current (DC) electricity. While a rectifier is an electronic device that converts AC voltage into DC voltage. In other words, it converts alternating current to direct current. According to the period of conduction, rectifiers are classified into two categories: Half wave rectifier and Full wave rectifier (Figure 6).

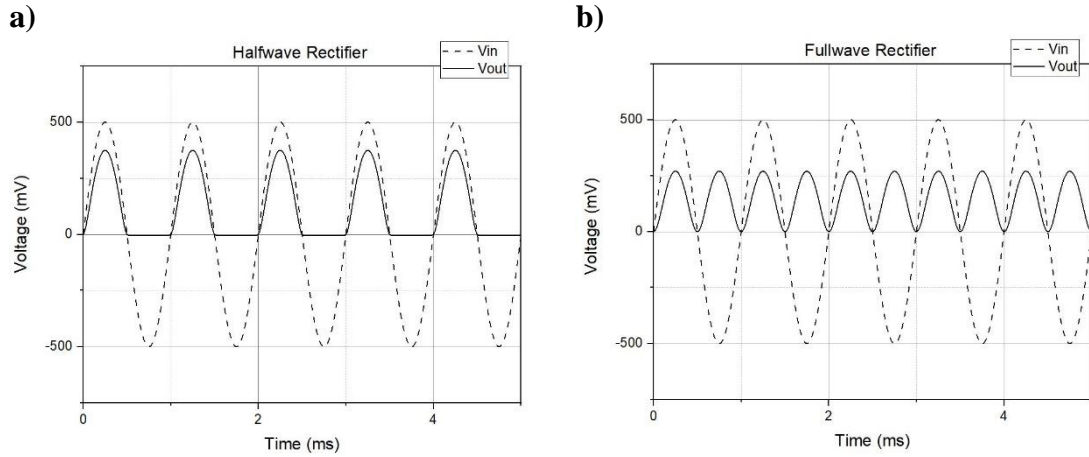


Figure 6. Types of rectifiers a) Half wave rectifier and b) Full wave rectifier.

The difference between half wave and full wave rectifier is that the half wave rectifier conducts for the positive or negative half cycle of the input signal and the full wave rectifier circuit conducts for both positive and negative cycles of the input signal. The DC output from the full wave rectifier is more stable than half wave circuits.

The rectennas are used in wireless power transmission systems that transmit power by radio waves. A simple rectenna element consists of a dipole antenna with an RF diode connected across the dipole elements. The diode rectifies the AC induced in the antenna by the microwaves, to produce DC power, which powers a load connected across the diode. Schottky diodes are usually used because they have the lowest voltage drop and highest speed and therefore have the lowest power losses due to conduction and switching.

4 SIMULATION STUDY

In this chapter, a study of the proposed circuits of the reference is made, to observe the rectification obtained for different voltage values and at high and low frequency. The study circuits are those observed in Figure 7.

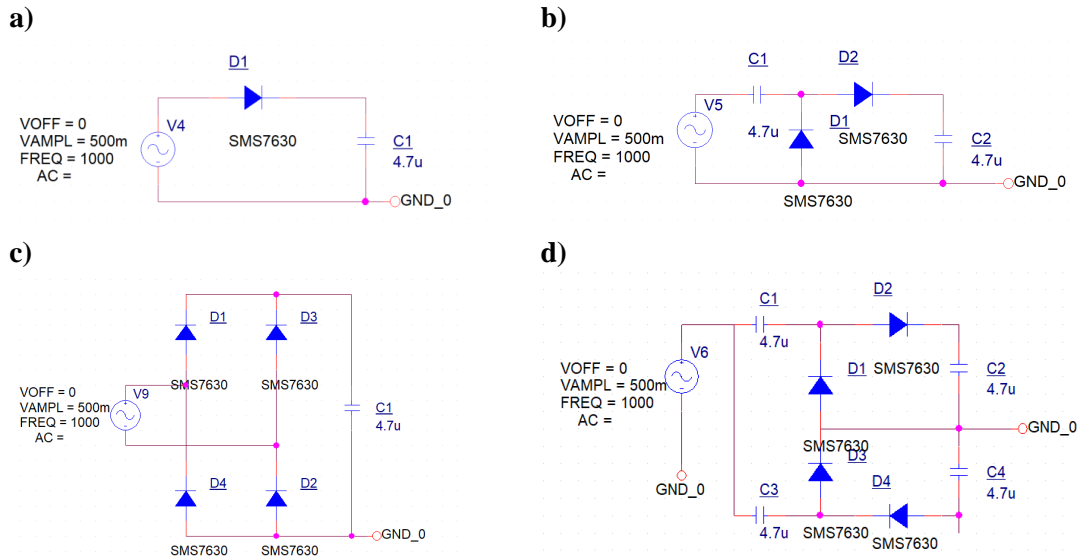


Figure 7. Study topologies a) Half wave rectifier, b) Voltage doubler, c) Full wave rectifier and d) Greinacher circuit.

The simulation environment used corresponds to the Orcad Pspice which allows the creation and documentation of electrical circuits. In order to simulate as accurately as possible, the Spice parameters of Annex 10.2 are used and forward bias current vs forward voltage is verified with data from the Schottky diode datasheet [8].

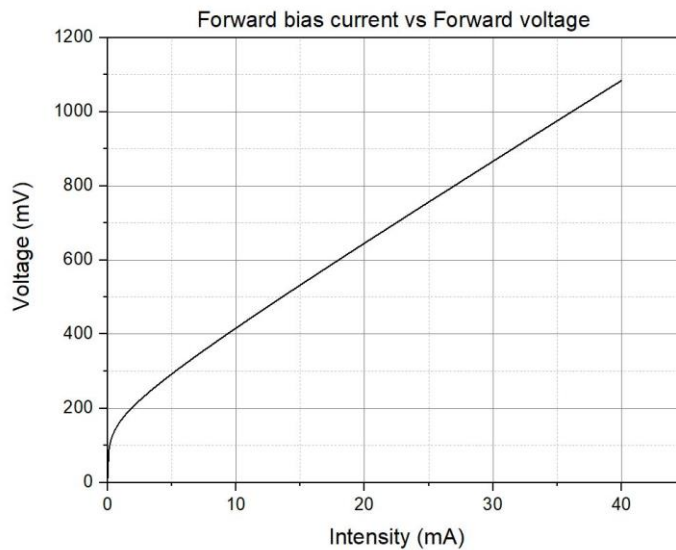


Figure 8. Forward bias current vs forward voltage simulated from the Schottky diode [8]

As shown, the minimum voltage required to start the current at the diode or barrier voltage (V_f) corresponds to approximately 150-200 mV. Next, the operation of each circuit is explained in detail.

Half wave rectifier:

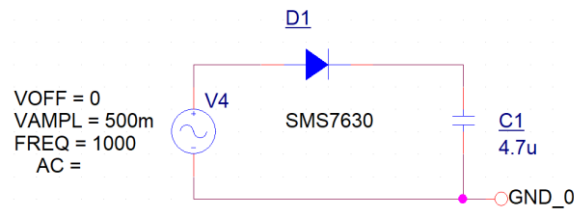


Figure 9. Schematic of a half wave circuit

During the positive half cycle the diode is forward biased and conduct current to the load. The current develop voltage across the load which has the same as the positive half cycle of the input AC signal voltage.

Alternatively during the negative half cycle of the input signal. The diode is reverse biased there is no current flow through the diode during this half cycle. There is no voltage drop across the load at the time. The result is that only the positive half cycle of the AC input voltage appears across the load, making the output a pulsating DC voltage.

Full wave rectifier:

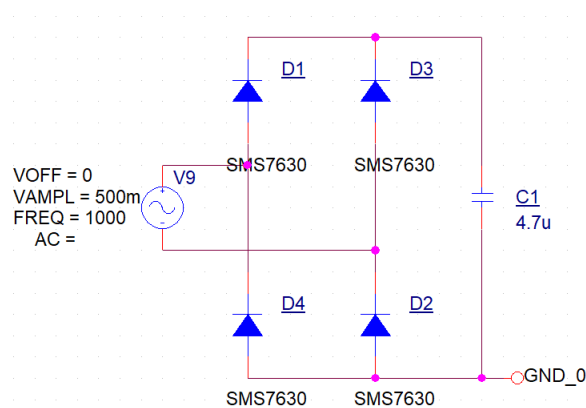


Figure 10. Schematic of a full wave bridge rectifier or bridge rectifier.

As shown in the schematic (Figure 10) of full wave bridge rectifier consist of 4 diodes under the condition in which 4 diodes are connected the called bridge circuit. So due to this type of circuit is named bridge rectifier.

When the positive half cycle of the supply goes, D1, D3 diodes conduct in a series while diodes D2 and D4 are reverse biased and the current flows through the load. During the negative half cycle, D2 and D4 diodes conduct in a series and diodes D1 and D3 switch off as they are now reverse biased configuration. Thus the direction of flow of current through the load remains the same during both half cycles of the input voltage, achieving a more stable output compared to the half-wave rectifier.

Generally, the DC output voltage of a rectifier circuit is limited by the peak value of its sinusoidal input voltage. But by using combinations of rectifier diodes and capacitors together we can effectively multiply this input peak voltage to give a DC output equal to some odd or even multiple of the peak voltage value of the AC input voltage. The circuits described above are called voltage multipliers and are explained below.[9]

Voltage doubler circuit:

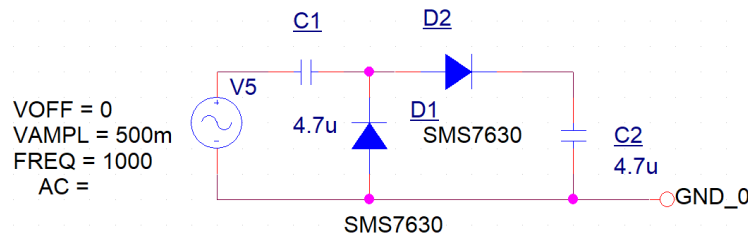


Figure 11. Schematic of a half-wave voltage doubler.

The circuit of the Figure 11 shows a half-wave voltage doubler. During the positive half-cycle of the input signal, the diode D1 conducts and the diode D2 is cut off, charging the capacitor C1 up to the peak rectified voltage i.e, V_m . During the negative half-cycle, diode D1 is cut off and diode D2 conducts across capacitor C1 is in series with the input voltage. Therefore the total voltage presented to capacitor C2 is equal to $2 V_m$ during the negative half cycle.

On the next positive half cycle, the diode D2 is non-conducting and the capacitor will discharge through the load. If no load is connected across capacitor C2, both capacitors stay charged at their full values (i.e, $C1=V_m$ and $C2= 2V_m$).

Greinacher circuit:

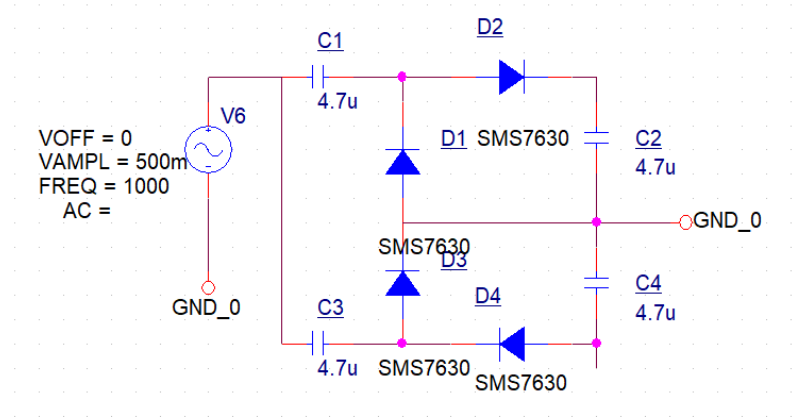


Figure 12. Schematic of a full wave series multiplier or Greinacher circuit.

The above circuit, known as Greinacher circuit, shows a basic symmetrical voltage multiplier circuit made up from two half-wave rectifier circuits. This type of voltage multiplier configuration is also known as a Full Wave Series Multiplier because each half-wave rectifier circuit is conducting in a different half cycle, the same as for a full wave rectifier circuit. Therefore, the voltage presented to the capacitor in each half-wave rectifier is equal to $2 V_m$, which gives a total voltage of $4V_m$.

4.1 ANALYSIS

A comparative graph between all the circuits described in Figure 7 is shown below, for an input voltage of 500 mV and a frequency of 1 kHz.

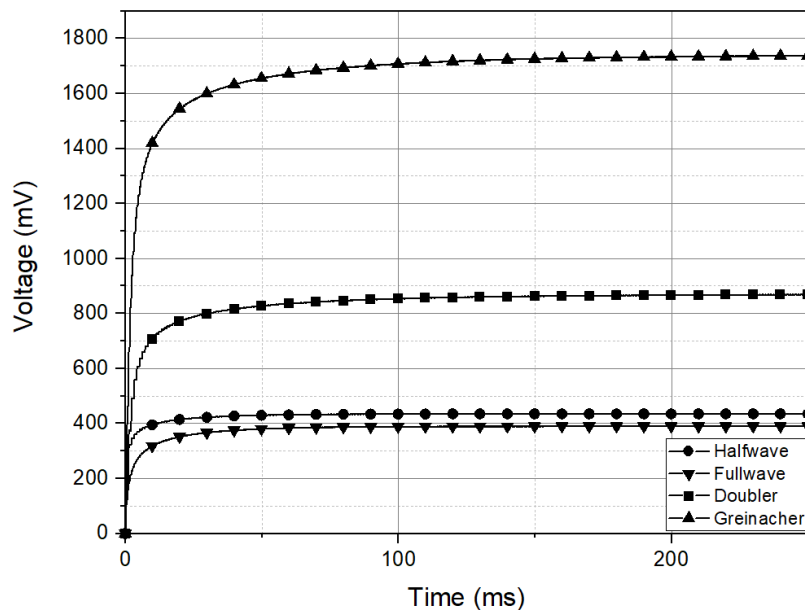


Figure 13. Comparison of the output voltages between study circuits in low frequency (1 kHz)

For a period of 250 ms at 1 kHz, it is shown that the Half-wave rectifier achieves a rectification of 430 mV, while the full-wave circuit is lesser with a rectification of 390 mV. On the other hand, the Voltage doubler circuit does not manage to double the input voltage to 1 V, but the voltage obtained is higher than the input, with approximately 870 mV. The Greinacher circuit, whose configuration is a stacked combination of two doublers, is estimated to double the output voltage of the voltage doubler, while achieves a voltage of 1.74 V.

The same study of the circuits for high frequencies is performed below in the Figure 14 for a frequency of 100 MHz. The study in high frequency is destined to the order of GHz, but due to the limitations of the software, a value of 100 MHz is selected for an optimal process.

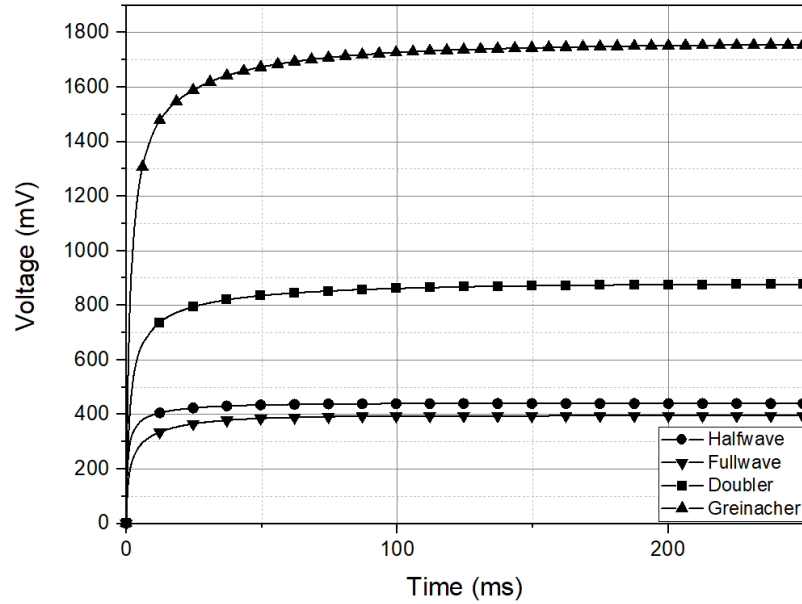


Figure 14. Comparison of the output voltages between study circuits in high frequency (100 MHz).

As can be seen in comparison to Figure 13, by increasing the operating frequency of the circuits at 100 MHz, the output potential is minimally increased.

Since the energy collection can be low, the behaviour of the circuits can be affected depending on the input that is obtained. This is due to the barrier potential operated by the Schottky diode, which is close to 200 mV as shown in Figure 8, which allows the current to flow.

For this reason, the circuits are excited for values in the range of the barrier potential, up to their breaking voltage corresponding to 2V, in order to observe the behaviour at the output of the circuits.

The data obtained in the graph below has been obtained by adding a 1k Ω load at the output for the half-wave and full wave rectifier, to observe the voltage drop that occurs in the diode.

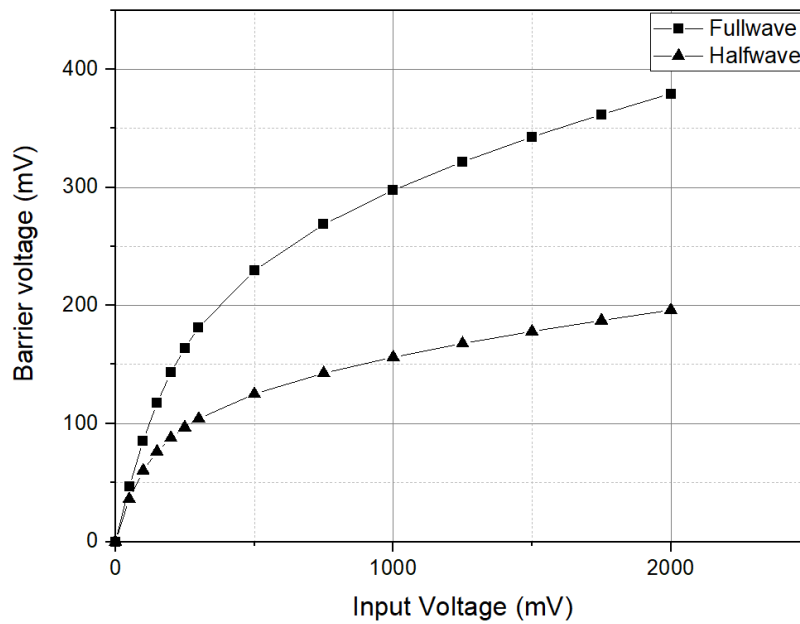


Figure 15. Representation of the voltage drop at the diode of the Half wave rectifier and Full wave rectifier.

As shown in Figure 15, the half-wave and full wave rectifiers have an identical behaviour to the observed in the forward bias current vs forward voltage of Figure 8. Therefore the behaviour of both circuits is proportional to the barrier voltage of the circuit and they are not modified by applying minimum voltages.

For the voltage multipliers, the above procedure cannot be performed because it can affect the operation of the circuit. Therefore, the accumulated load obtained on both multipliers is analysed to observe their operating conditions.

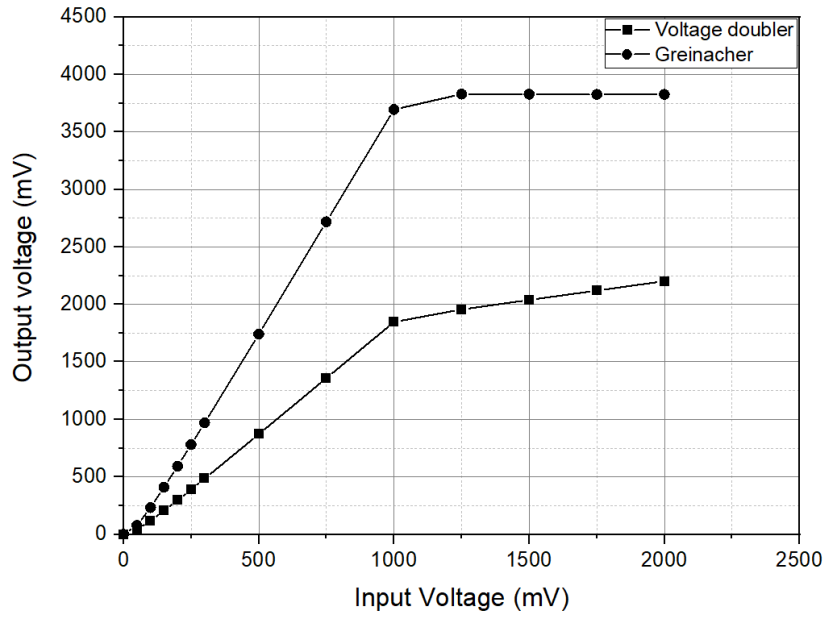


Figure 16. Representation of the output voltage of the multiplier circuits: Voltage doubler and Greinacher circuit.

The data obtained in Figure 16 show that the voltage multipliers require an input higher than 100 mV to surpass the rectified voltage. Also, the multipliers don't reach their respective output factors until a 500 mV input is applied. And finally it is observed that both circuits reach their maximum rectification level at 1V of input voltage.

Due to the restrictions seen in the voltage multipliers, half-wave and full wave circuits are more optimal for the application, because of their adaptability to low voltages, although they do not reach the rectification levels of the multipliers.

4.2 SCALABILITY

In this section, the combination of the previous circuits is studied in order to achieve a higher tension in the output and see its limits. Among the different circuit combinations, a parallel combination can be made that allows a higher load at the output, while a series combination allows the input voltage to be increased producing a faster load. Since the loading time is not a relevant factor in the study case, the cascade combinations of the circuits are applied.

From the referenced article [1], a cascade combination of 4 Voltage doublers is made as shown in the Figure 17.

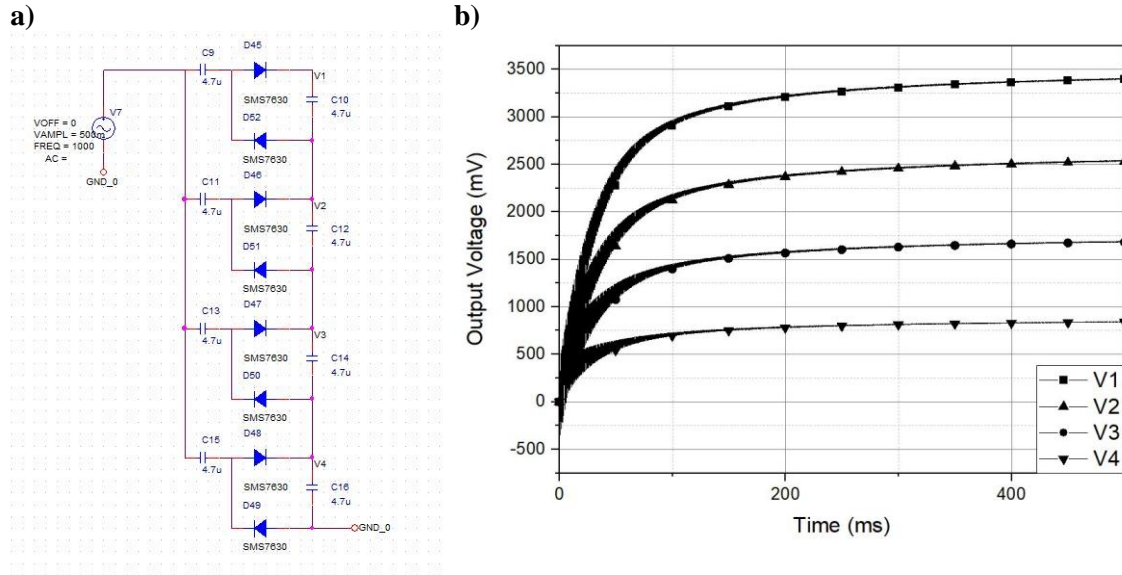


Figure 17. Representation of a) the scaled Voltage doubler circuit and b) the output voltage as a function of time.

Based on the application of the architecture, it is estimated that each doubler should acquire approximately 800 mV as obtained in the Figure 13, so that it should obtain about 3.2V. As can be seen in the Figure 17, applying an input voltage corresponding to 500 mV causes the accumulated voltage with all capacitors to reach approximately 3.4V.

The voltage produced by a voltage multiplier circuit is in theory unlimited, but due to their relatively poor voltage regulation and low current capability there are generally designed to increase the voltage by a factor less than ten. Also, voltage multipliers usually supply low currents to a high-resistance loads as the output voltage quickly drops away as the load current increases.

Concerning the other configurations, the results of cascade combinations are not feasible, due to the polarization of the diodes being affected by the addition of these stages.

5 IMPLEMENTATION

In the previous section, it's described the behaviour of each circuit using the Orcad Pspice simulation tool. This section explains the assembling process of the circuits, the tools and equipment used, the measurement procedures and results for high and low frequency.

The study for low and high frequency is performed separately due to the complexity to monitor the results. When operating in high and low frequency simultaneously, it's not possible to characterize its effects separately. The only way to evaluate it is observing the power level at the output of the circuits.

5.1 FABRICATION

In this part, the schematics of the Figure 7 are implemented in circuits, bearing in mind, its dimensions reduction in order to minimize the complexity of the circuits and suppress the ohmic loss.

To realise the montage of the circuits, a test board with several points is used in order to sense the input and output voltage. The connections between the components and vias are established with test points, soldered using lead free tin with a temperature of 350°C. To perform the assembling process a Leica microscope and a JBC solder station are used, as it's shown in the following figure (Figure 18).



Figure 18. Instrumentation used for the fabrication of the circuits: a Leica microscope and a JBC solder station.

The components used are Surface Mount Device (SMD) due to the reduced dimensions compared to Through Hole Devices (THD) for diodes or electrolytic capacitors which can add ohmic loss to the measurements. $4.7\mu\text{F}$ standard value capacitors are used in the circuits, which quite commonly form part of harvesting systems.[10] The capacitor's dimensions and packaging, which is 0805mm, is selected precisely, bearing in mind its electric specifications, such as a low Equivalent Series Resistance (ESR).

The equivalent series resistance of a capacitor is the internal resistance that appears in series with the capacitor. Low ESR capacitor devices minimize capacitor losses, increase the efficiency and stability of the power supply. In addition, it also helps to reduce the output ripple voltage.

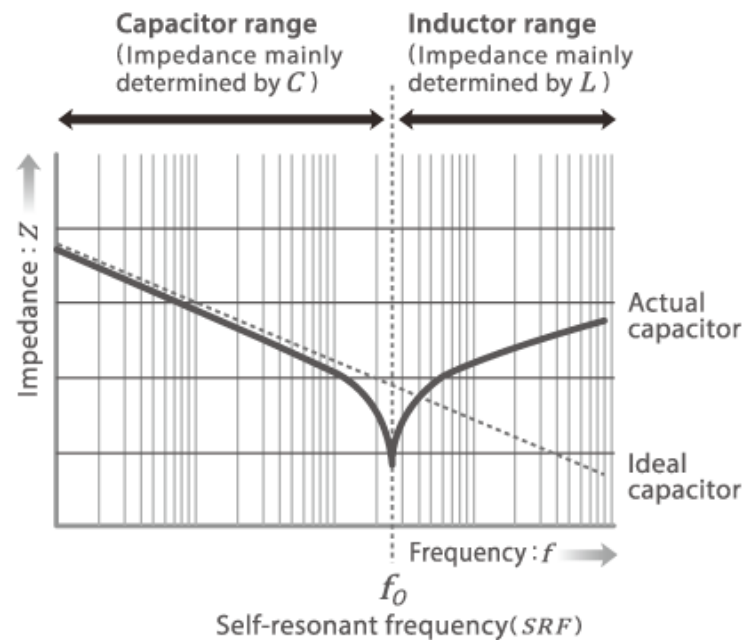


Figure 19. Impedance vs frequency response characteristic for a capacitor.[11]

As it can be seen in the Figure 19, at frequencies above the self-resonant frequency f_0 , the operation of the capacitor is dominated by the parasitic inductance causing to lose its properties as a capacitor.

The Schottky diodes is used due to its high sensibility, low threshold voltage and frequency response which covers our operation range easily.

Finally, to verify that the assembling process has been performed flawlessly, a multimeter is used to check the connections between the components, vias and connectors. It's also important to verify the Schottky diode forward voltage, because during the soldering process this component can break easily. The final result of this process are the circuits shown in the Figure 20.

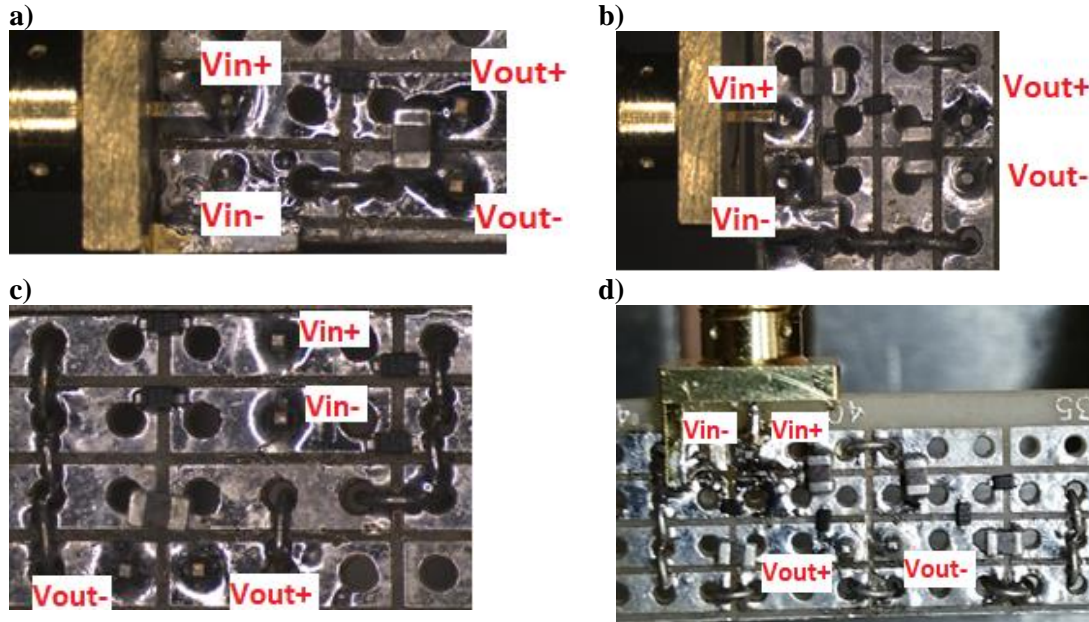


Figure 20. Implementation of a) the Half wave rectifier, b) the Voltage doubler circuit, c) the Full wave rectifier and d) the Greinacher circuit (see the schematics circuit in Figure 7).

5.2 STUDY IN LOW FREQUENCY

Starting from the results obtained in Section 4, it's proceed to extract the voltage at the output load of the study circuits. For this purpose, an oscilloscope is used as a power supply and for the measuring.

To perform a test on previously mounted circuits, a power supply is required that works on the operating voltages of the circuits and at low frequencies. In order to proceed with this measurements, monitoring the output voltage of each circuit is also required. Therefore, the equipment used in this section is a digital oscilloscope InfiniiVision.DSOX3014A of Agilent.

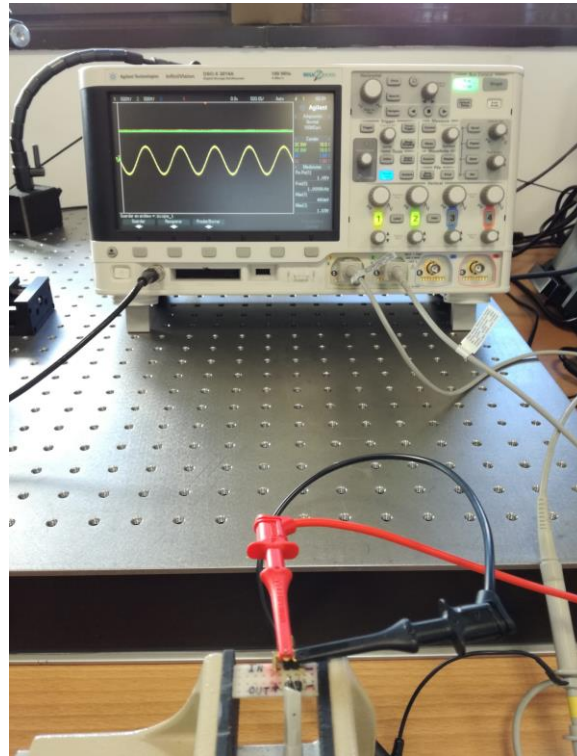


Figure 21. Instrumentation used for low frequency characterization: a digital oscilloscope.

To simulate the input voltage of an antenna, as is done in the simulations of the previous section, a sinusoidal signal is introduced with a frequency of 1 kHz. The signals amplitude is 1 V_{pp}, equivalent to 500 mV.

The result of this test should be practically identical to the results obtained in the simulations. In order to prove that, two points of the circuit (Figure 20) are sensed with the oscilloscope using a probe 100:1. Also, this study provides a reliable way to verify that the previously made manufacturing process is correct.

The results obtained from this study are captured from the oscilloscope, which are shown at the Figure 22.

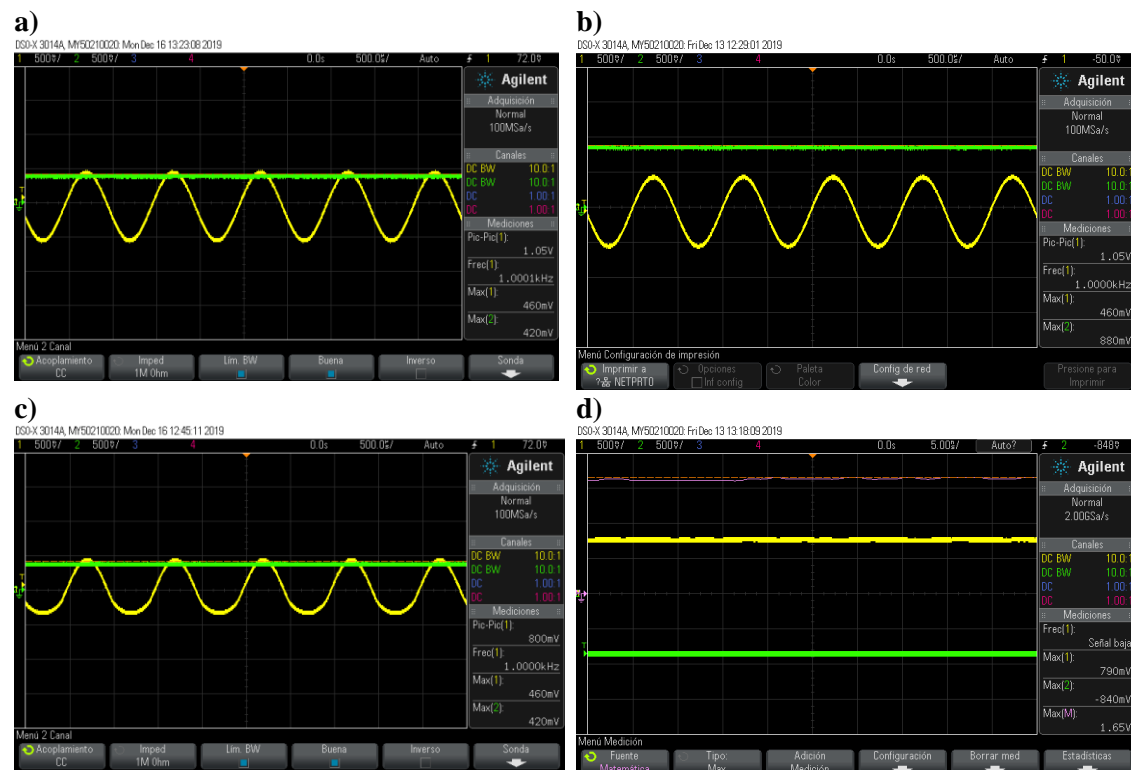


Figure 22. Results obtained in the oscilloscope for an input of 500 mV at 1 kHz in a) the Half wave rectifier, b) the Voltage doubler, c) the Full wave rectifier and d) the Greinacher circuit.

As it can be seen in the previous captures, the experimental result for an input of 500 mV is practically identical to those obtained in the simulations. As seen in the simulations, among all the study circuits, the best option is the Greinacher circuit due to the amount of voltage obtained at the output.

To determine the operation of the circuits at low voltages, the minimum voltage of 100mVpp is applied to the oscilloscope, corresponding to 50mV, as shown in the Figure 23.

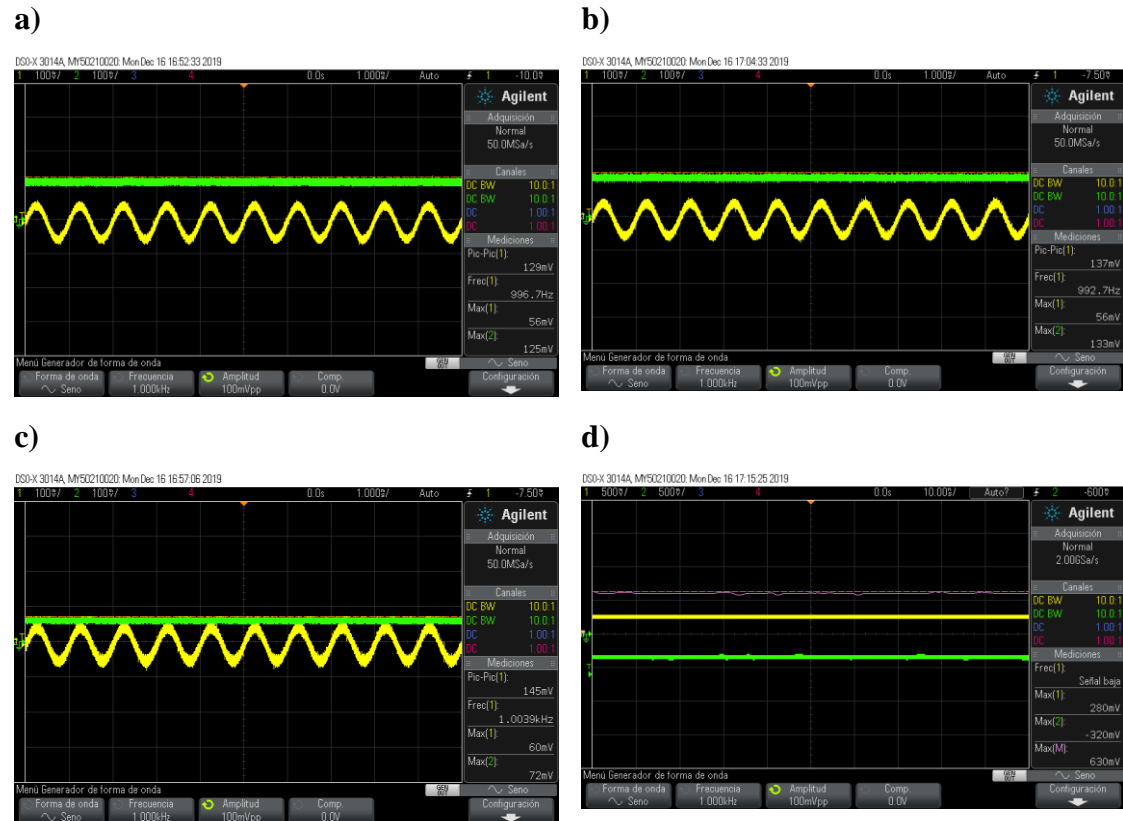


Figure 23. Results obtained in the oscilloscope for an input of 50 mV at 1 kHz in a) the Half wave rectifier, b) the Voltage doubler, c) the Full wave rectifier and d) the Greinacher circuit.

Despite the fact that the input voltage is lower than the barrier voltage (V_{γ}), the Voltage doubler and the Full wave rectifier behave correctly. Nevertheless, the Half wave rectifier and the Greinacher circuit obtain a vastly higher voltage than the input, which is not corresponding to the simulated or expected.

5.3 STUDY IN HIGH FREQUENCY

In this section, the different voltage measurements carried out in high frequency for the study circuits are explained.

To test mounted circuits, a power supply capable of operating at high frequencies close to 2.4 GHz is required. For this purpose, a network analyzer is used.

A network analyzer is an instrument capable of analyzing the properties of electrical networks, especially those properties associated with the reflection and transmission of electrical signals. The basic architecture of a network analyzer involves a signal generator, a test set and one or more receivers.

The network analyzer model used is an E8357A of Agilent, which is able to work from 300 Hz to 6 GHz. It is used applying powers in dBm in the input of the circuits for a specific frequency. To observe the power introduced by the network analyzer, a spectrum analyzer is used.

A spectrum analyzer is an electronic measuring equipment that allows to visualise on a screen the spectral components in a frequency spectrum of the signals present in the input, being able to be any type of electric, acoustic or optical waves. The spectrum analyzer model used is a Rohde & Schwarz FSL, which is able to work from 9 kHz to 6 GHz.

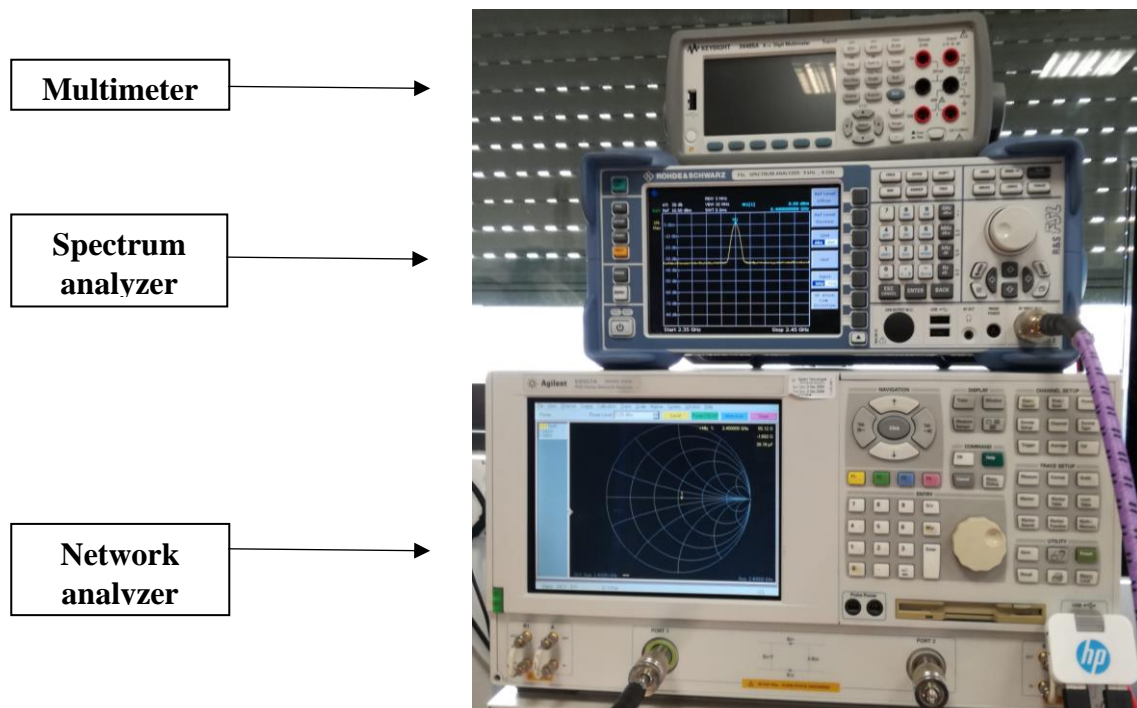
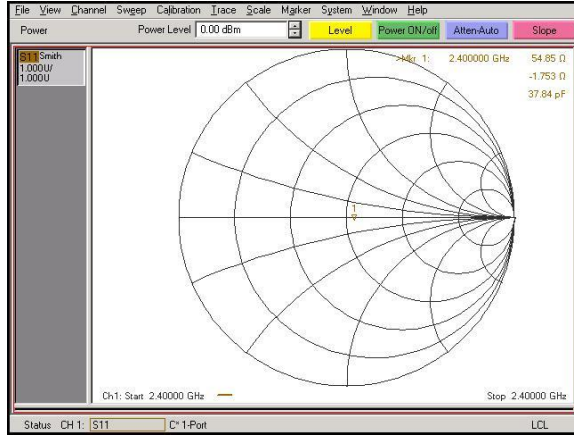


Figure 24: Instrumentation used for high frequency circuit characterization: a Multimeter, a Network analyzer and a Spectrum analyzer.

The network analyzer is set to the frequency range to operate at the Wi-Fi frequency of 2.4 GHz. In the same way, the same procedure is done with the spectrum analyzer to observe the power introduced by the network analyzer. In order to sync the sampling of both devices, their triggers are connected to each other, as shown below.

a)



b)

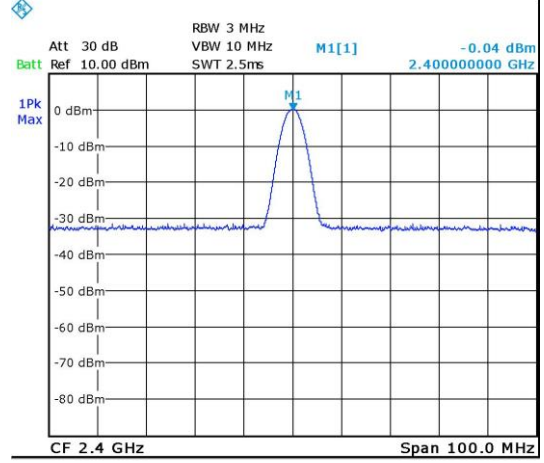


Figure 25. Calibration at 0 dBm of a) the Network analyzer with b) the Spectrum analyzer.

As can be seen in the previous images, an input power of 0 dBm is introduced from the network analyzer, but the spectrum analyzer shows that the maximum peak corresponds to -0.04 dBm. Also note that the network analyzer shows the input impedance of the spectrum analyzer of approximately 55 Ω , when both devices operate with an impedance of 50 Ω . One of the effects could be for the accuracy of both devices and the harness used in the measurements. The network analyzer's reference level for input power calibration is modified to minimize the previous effect. The ideal procedure would require a specific power calibrator which is not available.

From the power introduced by the network analyzer, it can be extrapolated to obtain the equivalent introduced voltage. This requires taking into account the circuit impedance, which is obtained with the network analyzer (as shown in Figure 25a) by performing the impedance module function. In order to obtain the input voltage of each circuit, the following equations are computed:

$$P(W) = 10^{\frac{P(dBm)}{10}} \cdot \frac{1W}{1000mW} \quad (1)$$

$$V_{RMS} = \sqrt{\frac{P(W)}{R}} \quad (2)$$

$$V = V_{RMS} \cdot \sqrt{2} \quad (3)$$

Both, the impedance and the accumulated load, change according to the power introduced in the input. Consequently, a manual sampling of the input power is performed while extracting the real and imaginary impedance of the network analyzer, and the accumulated voltage at the circuit load with a multimeter. Due to the impedance introduced by the multimeter, the data extraction is performed separately and after each measurement the accumulated load is discharged.

In the high frequency study, an oscillation between the values of the impedance of the circuits was considered, so that a trendline has been drawn with the data obtained. The results extracted from using a network analyzer as a power source for high frequency are shown below:

Half wave rectifier:

In the performance of the high frequency study for the half-wave rectifier, the results obtained indicated a considerable oscillation in the measurement of the accumulated load at the circuit output that made it difficult to consider a specific value. Among these results, an accumulated charge with negative values was reported, which is considered an unacceptable value. Although the components of this circuits were working as expected, the result was the same even repeating the implementation of this half wave circuit. Due to this reason, the study could not be carried out for this type of circuit.

Full wave rectifier:

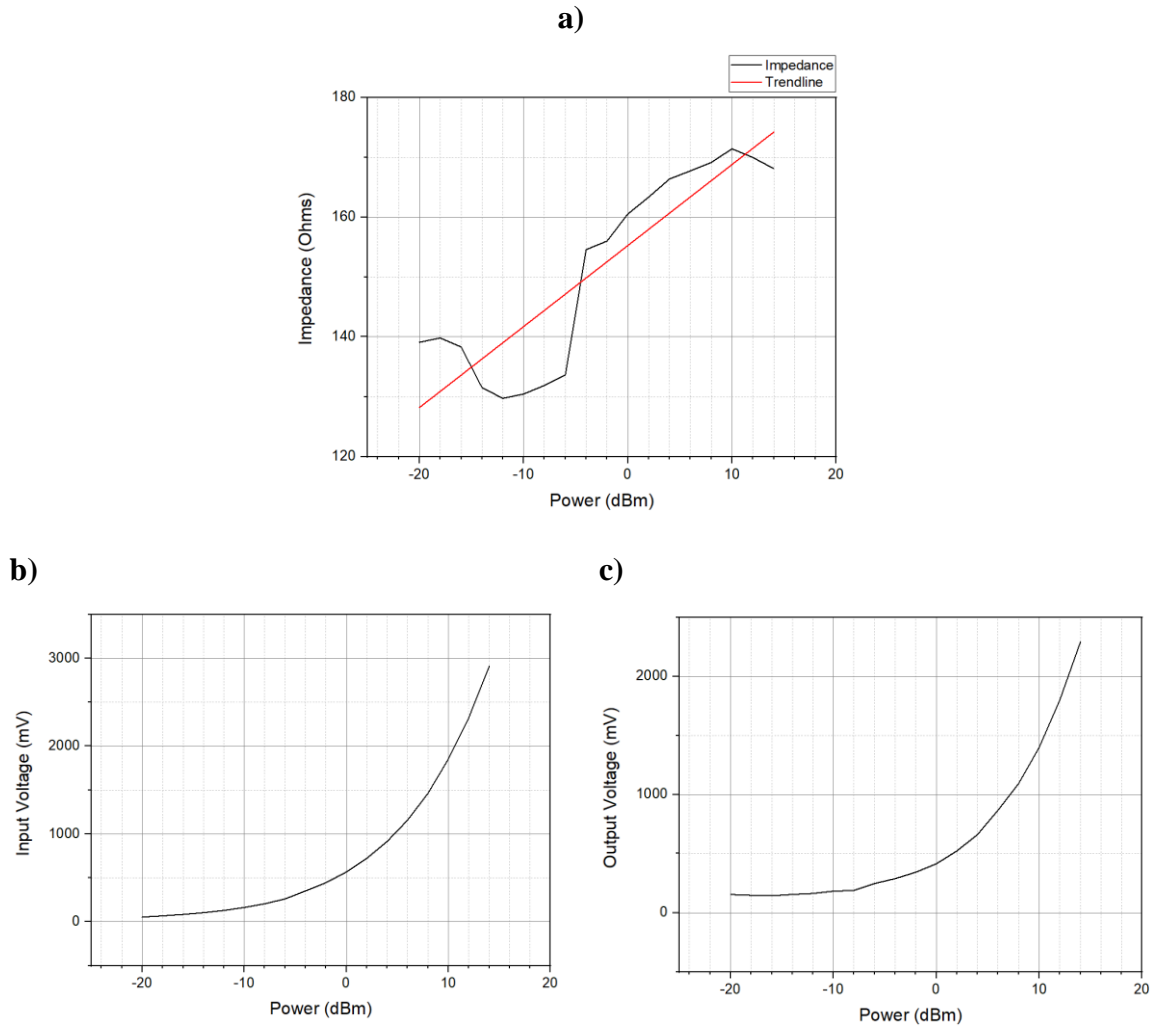


Figure 26. Representation of a) the impedance, b) the input voltage and c) the output voltage of the Full wave rectifier respect to the power introduced.

For the full wave rectifier in Figure 26, an impedance variation between 130-170 ohms is observed, which increases as a function of the power input. The power introduced so that the circuit can operate properly is in -8 dBm that corresponds approximately to 200mV. For lower values, the circuit would be within the range of the barrier voltage, where it typically fails to operate correctly.

Voltage doubler circuit:

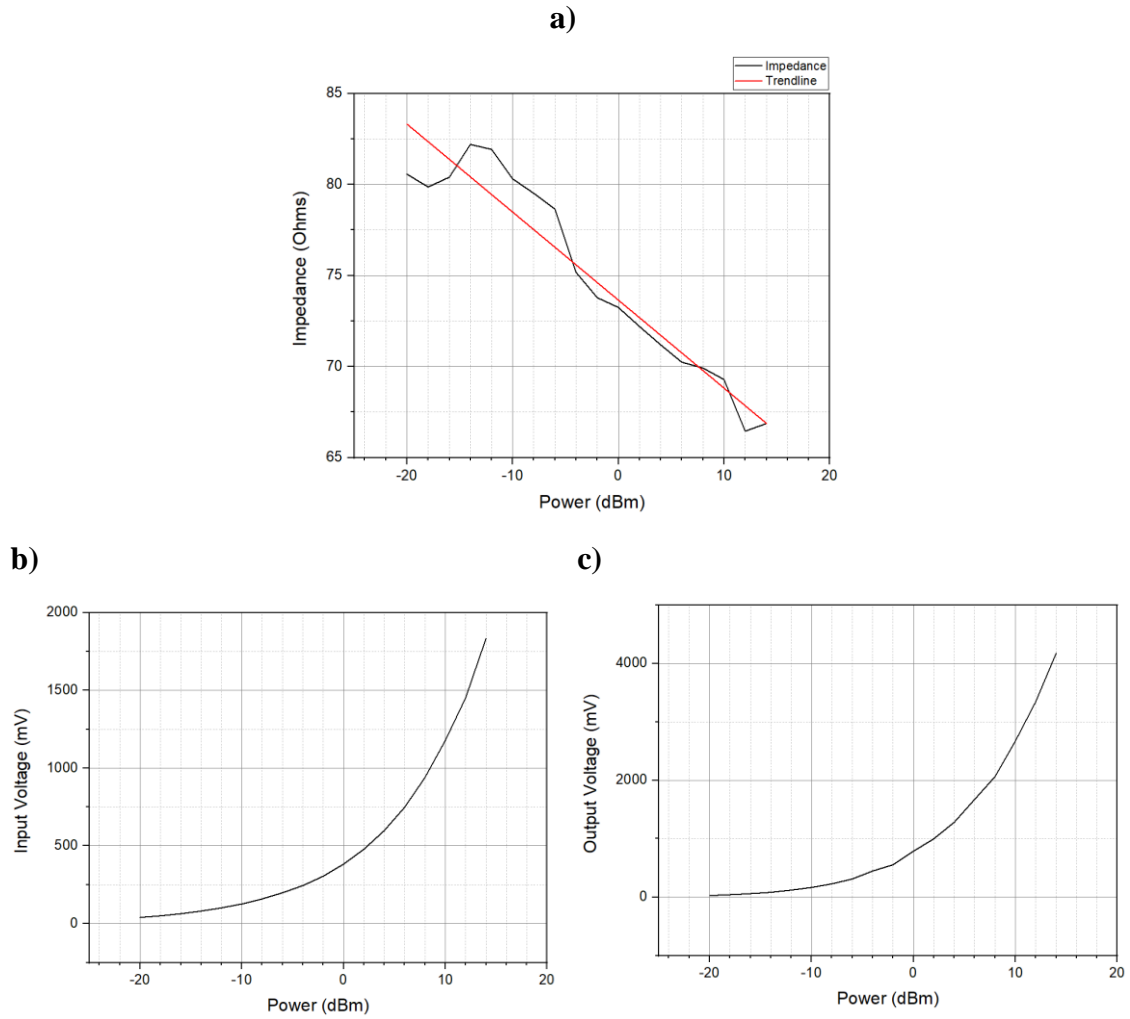


Figure 27. Representation of a) the impedance, b) the input voltage and c) the output voltage of the Voltage doubler circuit respect to the power introduced.

The data obtained from the voltage doubler in Figure 27 demonstrates that the circuit impedance matches 65-80 ohms, which decreases as the introduced power rises. Concerning the accumulated load, the voltage doubler for powers lower than -6 dBm which equivalent to 200 mV, cannot operate correctly, doubling the introduced voltage. On the other hand, for power levels higher than -6 dBm, this design operates correctly.

Greinacher circuit:

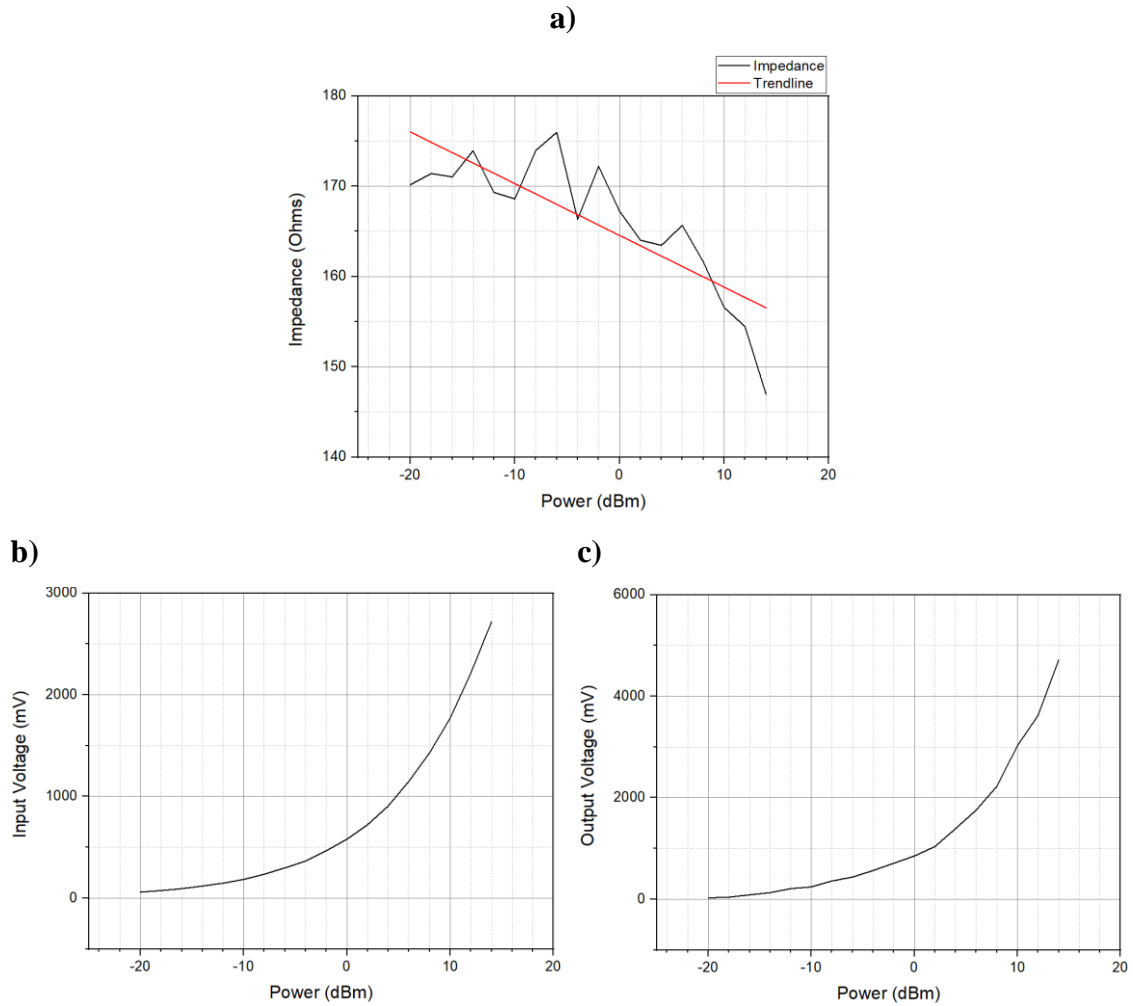


Figure 28. Representation of a) the impedance, b) the input voltage and c) the output voltage of the Greinacher circuit respect to the power introduced.

Finally, for the Greinacher circuit of the Figure 28, it is observed that its impedance oscillates between 145-175 ohms, where the impedance decreases according to the power introduced. Regarding the accumulated load of the circuit, it is estimated that it has to be obtained around 4 times the input voltage, but the maximum that is obtained is to duplicate the voltage for powers higher than -4 dBm approximately.

It can be concluded from the obtained data that the Half wave rectifier and the Greinacher circuit do not function correctly. On the other hand, both the Voltage doubler and the Full wave rectifier operate around 200 mV where the full wave rectifier operates in the range of the barrier voltage and their losses are lower in consideration of the losses of the other two circuits. Due to the impedance mismatch that can exist in the whole circuit respect the input of the measurement devices, the results vary in comparison with the simulated and expected ones. Therefore, it is concluded that the full wave rectifier is the most suitable for high frequency.

6 NON-LINEARITY IN HIGH FREQUENCY

Working at high frequencies and low voltages, the devices do not behave in the ideal way. Capacities cease to behave like a capacity and as frequency increases it behaves like an inductance (Figure 19).

The main reason why in the previous section the results related to high frequency are not as expected, is due to working with non-linear devices and inside the barrier voltage (V_j) of the diodes. The diode has other non-ideal features depending on the frequency at which it is working, there is a small signal model, for high frequencies, of the order of GHz, formed by a capacitive element and a parasitic impedance (Figure 29) that can affect the polarization of the diode.

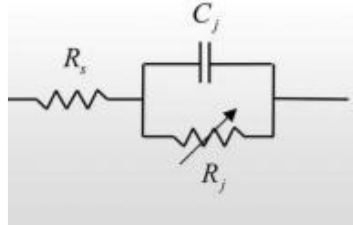


Figure 29. Small-signal model of a diode in high frequency.[5]

Also, design losses can occur due to parasitic capabilities caused by the thickness of the tracks and their proximity.

6.1 HARMONIC DISTORTION [5]-[6]

This effect does not only occur at high frequencies, it is at all frequencies. The system is non-linear, so that the power introduced in f_0 is divided into harmonics ($f_0, 2f_0, 4f_0 \dots$) (Figure 30).

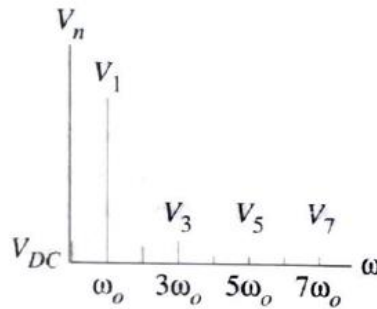
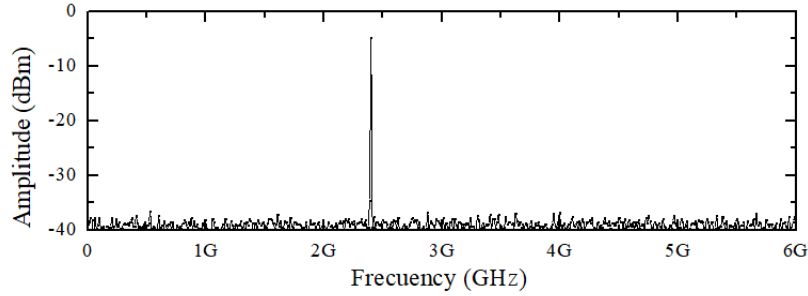


Figure 30. Example of harmonic distortion seen in the frequency domain of the output and the distortion components.[12]

For this reason it is not required to introduce an impedance adaptation for the fundamental frequency due to it contains a fraction of the initial frequency, as it's observed in the following graphs.

a)



b)

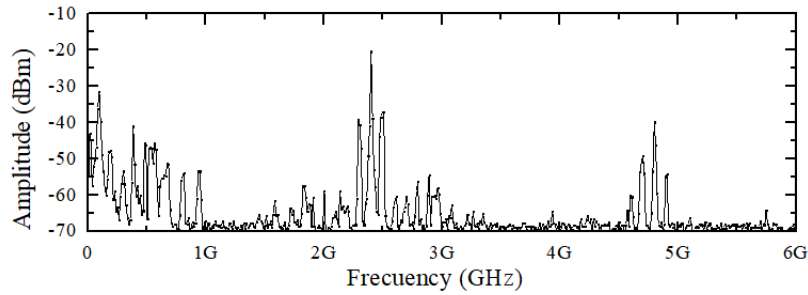


Figure 31. a) Delta sent in $f_0=2.4\text{GHz}$. b) Decomposition of the delta at the output of the rectifier.[5]-[6]

When dealing with non-linear systems, the entire spectrum should be considered. In such a way that it is not considered necessary to adapt impedances if only the power is considered.[6]

6.2 RESOLUTION IN HIGH FREQUENCY

As an alternative solution to perform the study in high frequency, the load is modified so as to operate better at high frequency as the schematic of the harvester system, seen in the Figure 4. The implementation of a $0.1\mu\text{F}$ capacitor in parallel is practically unaffected to the total load of the circuit.[13]

The same procedures described in the section are used for development, testing and high and low frequency studies.

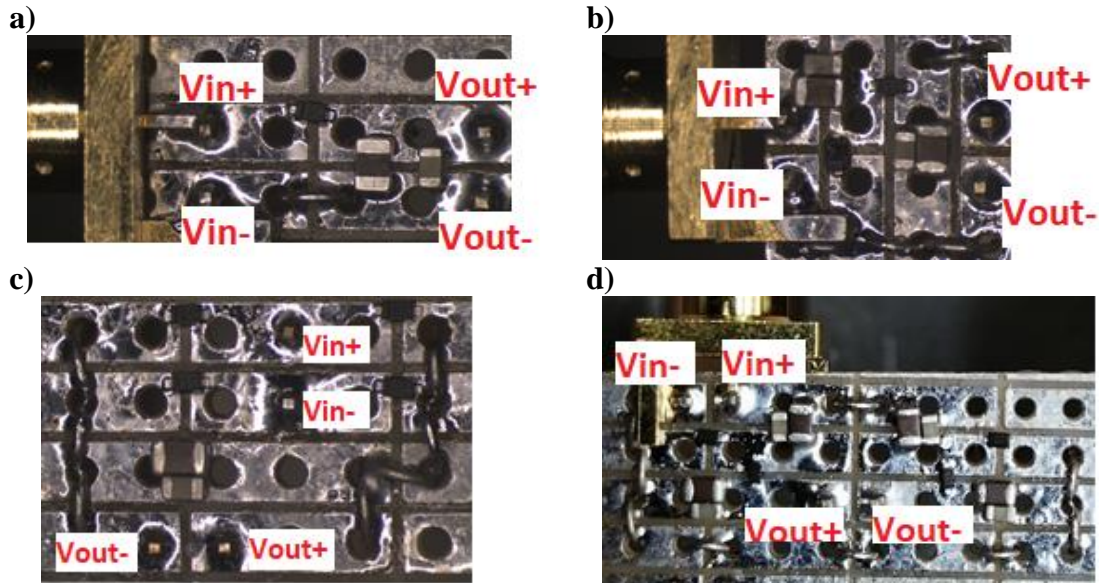


Figure 32. Implementation of a) the Half wave rectifier, b) the voltage doubler circuit, c) the Full wave rectifier and d) the Greinacher circuit, modified by adding a parallel capacitor at the output of each circuit.

The assembling procedure of the Figure 32 is identical to the Figure 20, it has not required to modify the allocation of components and paths for the addition of parallel capacity.

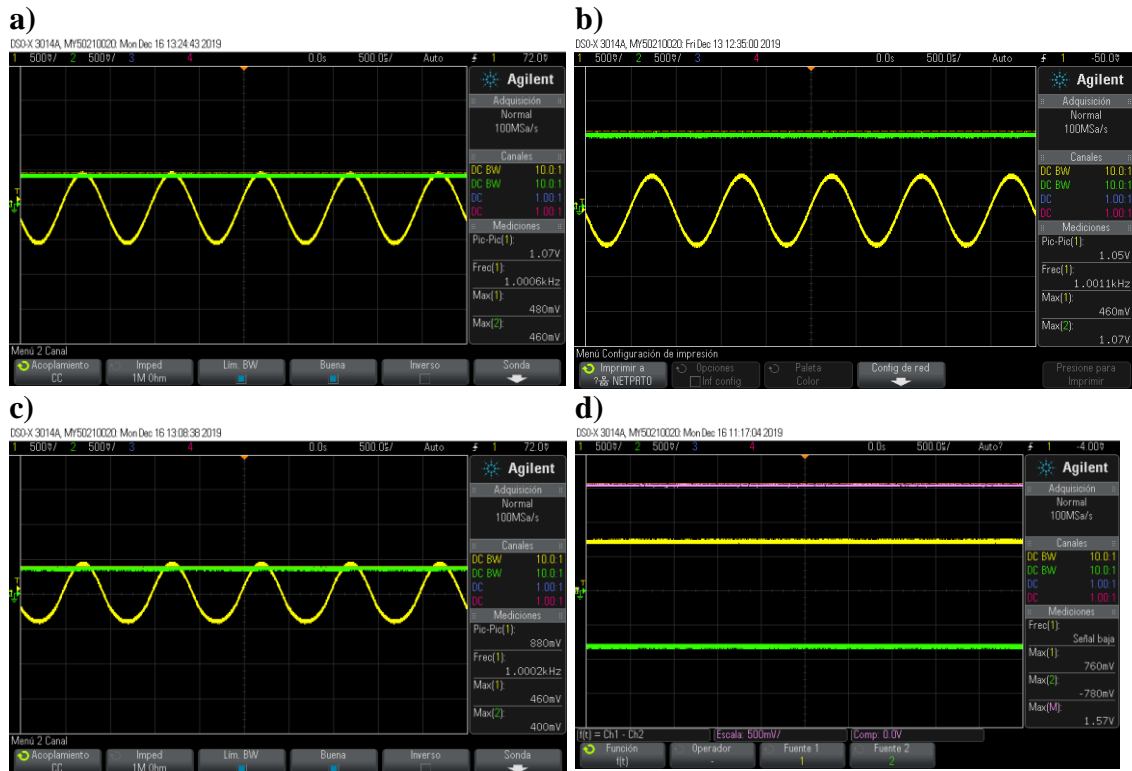


Figure 33. Results obtained in the oscilloscope for an input of 500 mV at 1kHz of a) the Half wave rectifier, b) the Voltage doubler circuit, c) the Full wave rectifier and d) the Greinacher circuit, modified by adding a parallel capacitor at the output of each circuit.

In the case of low-frequency studies, the addition of this component does not affect the output as shown in the Figure 33. As mentioned above, the addition of a lower capacity in parallel to a higher capacity does not affect the resulting load at low frequency. Which can be related with the 4.7 μ F resonance at lower frequency in comparison with the added capacitor.

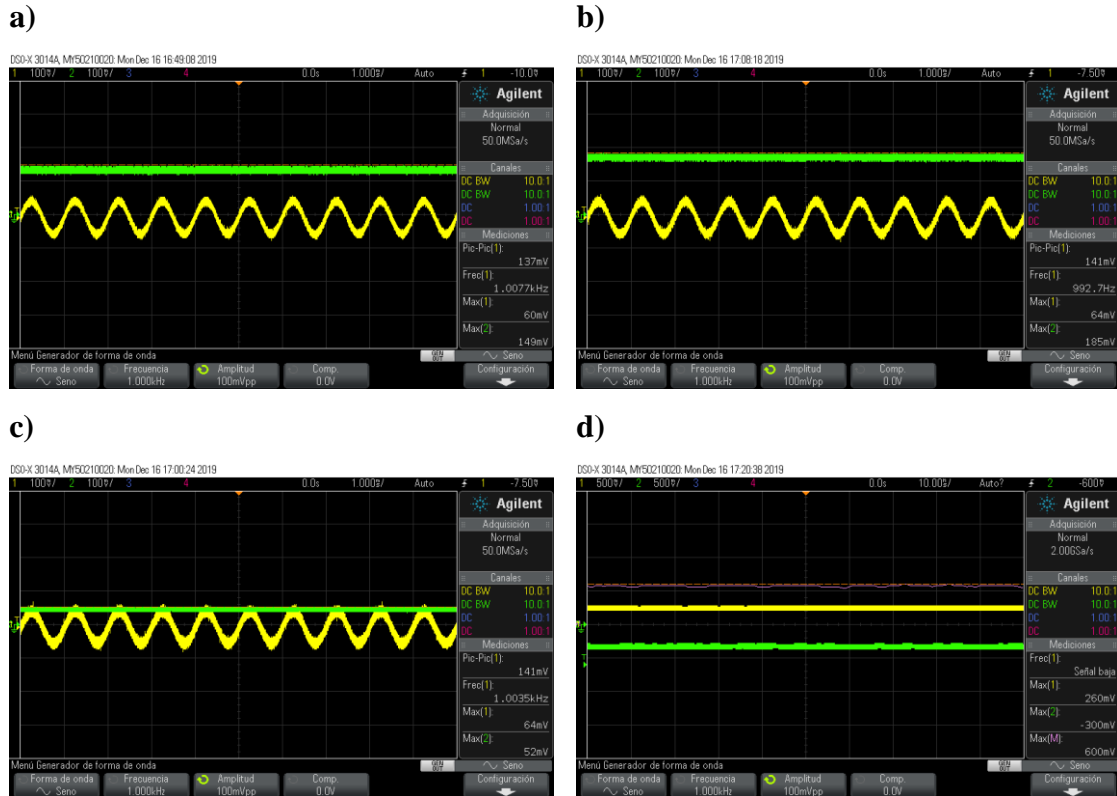


Figure 34. Results obtained in the oscilloscope for an input of 50 mV at 1kHz of a) the Half wave rectifier, b) the Voltage doubler circuit, c) the Full wave rectifier and d) the Greinacher circuit, modified by adding a parallel capacitor at the output of each circuit.

As in the previous section, the circuits are forced to operate at the minimum voltage that can be provided by the oscilloscope in such a way as to observe if their behaviour is still the same, as shown in Figure 23. Although the same circuits have been performed again, the same results are obtained as in Figure 34. Both, the voltage doubler and the full wave rectifier, work properly while the others don't.

Hence, the high frequency analysis is performed by applying the network analyzer.

Half wave rectifier:

In spite of the modifications in the circuit to improve the high frequency behaviour, no conclusive values are obtained for this type of circuit in the same way that in the previous section. Therefore, the use of the half-wave rectifier for high frequencies is rejected.

Full wave rectifier:

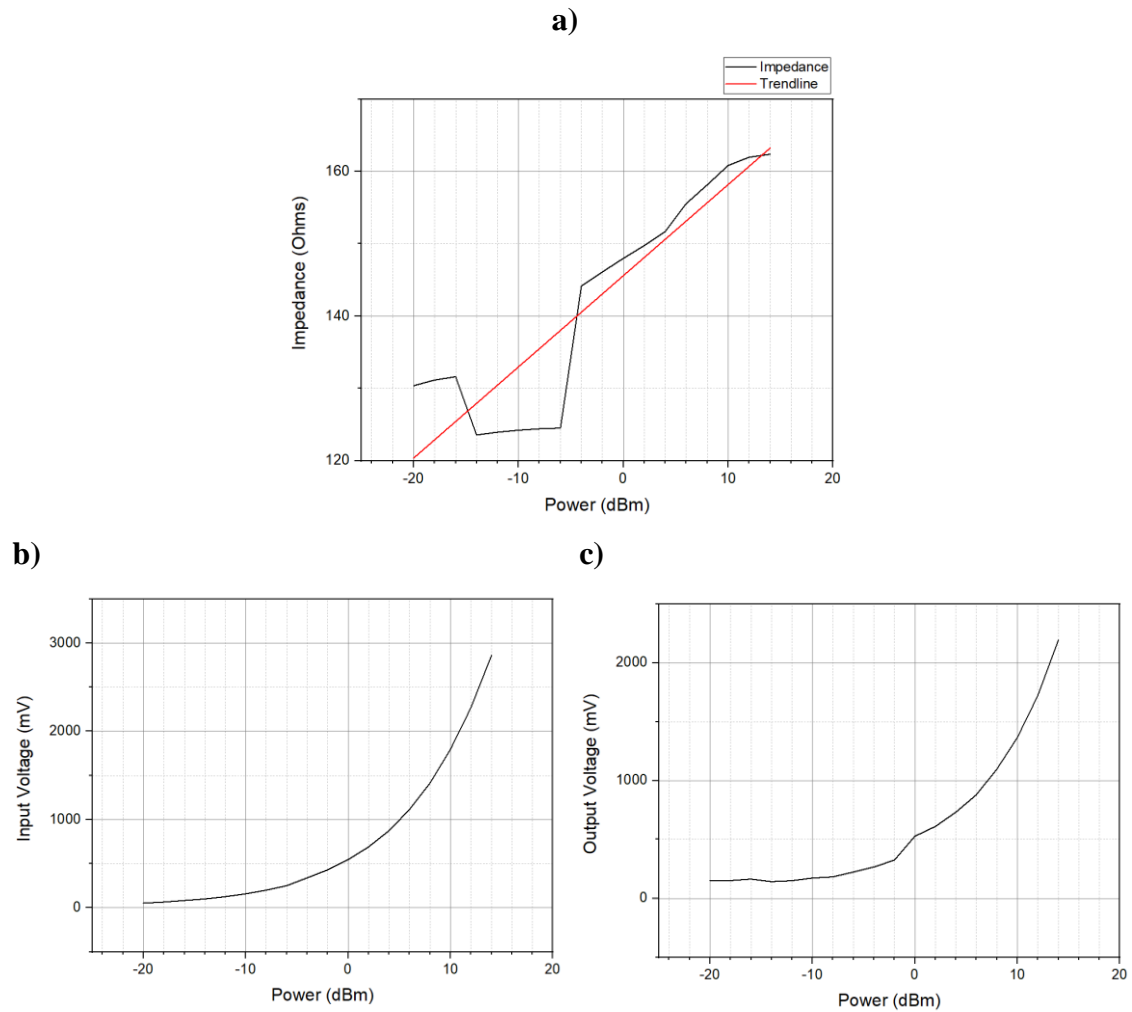


Figure 35. Representation of a) the impedance, b) the input voltage and c) the output voltage of the Full wave rectifier respect to the power introduced, modified by adding a parallel capacitor at the output of each circuit.

The following results are product of the analysis of full wave circuit (Figure 35) in high frequencies. As it can be seen, the results are pretty similar to the obtained in the previous study. Full wave rectifier impedance oscillates between 120-160 ohms, increasing as a function of power. The minimum power input for the circuit to work properly corresponds to -8 dBm, which corresponds to a voltage of approximately 200 mV.

Voltage doubler circuit:

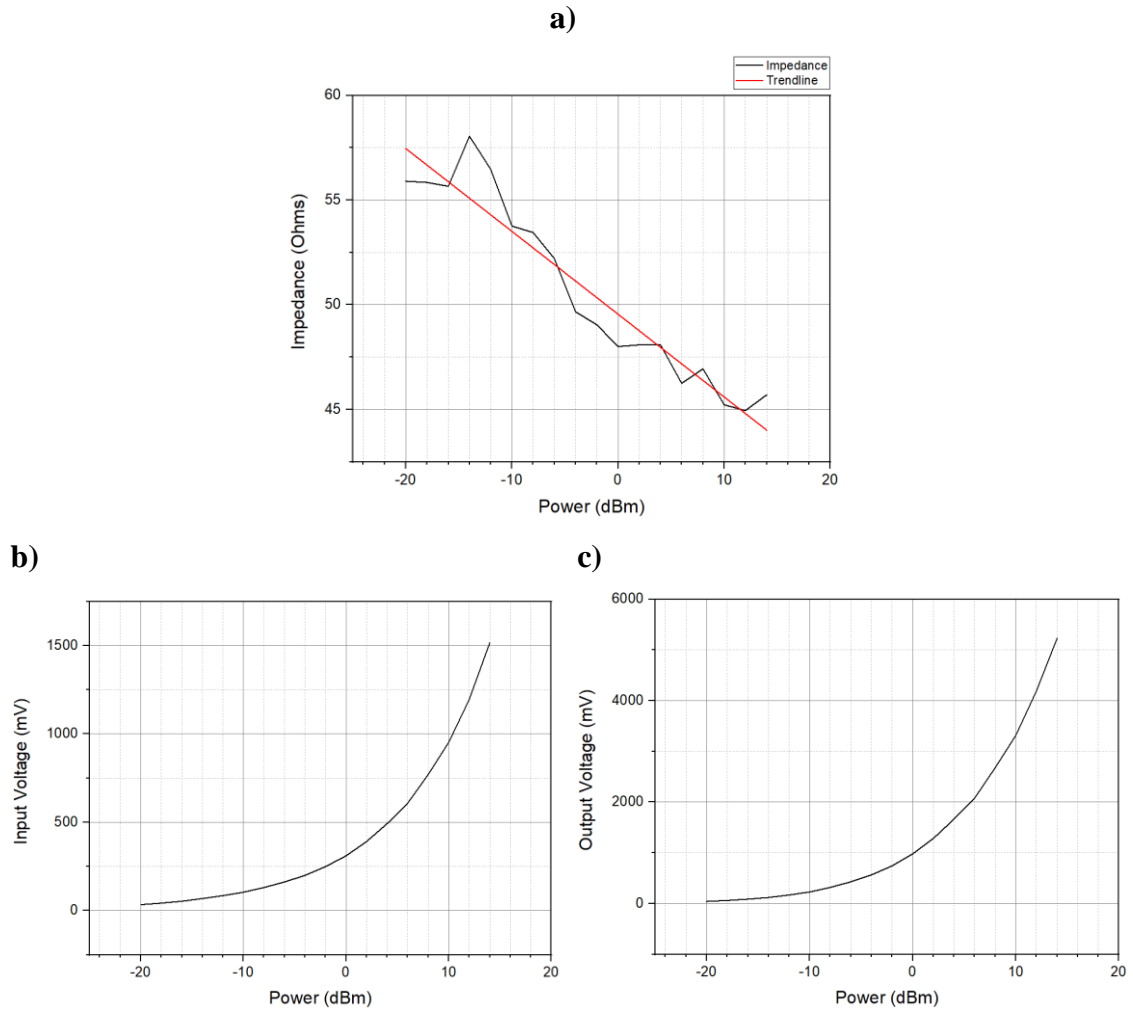


Figure 36. Representation of a) the impedance, b) the input voltage and c) the output voltage of the Voltage doubler circuit respect to the power introduced, modified by adding a parallel capacitor at the output of each circuit.

The high frequency Voltage doubler results (Figure 36) show that the circuit impedance corresponds to 45-55 ohms and it decreases as a function of the input power. In contrast to the measurement shown in Figure 27, the voltage doubler operates correctly for powers higher than -14 dBm, which corresponds to approximately 70 mV.

Greinacher circuit:

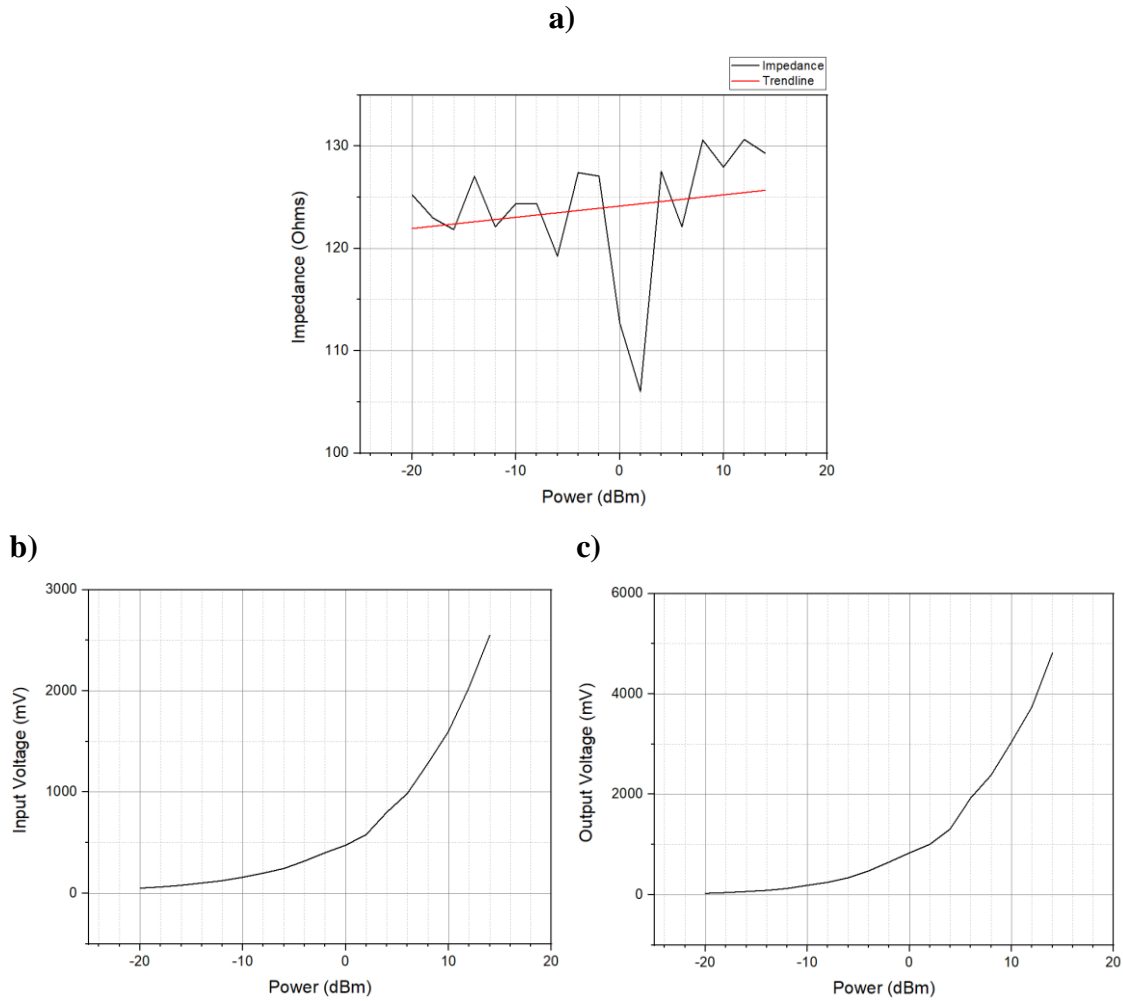


Figure 37. Representation of a) the impedance, b) the input voltage and c) the output voltage of the Greinacher circuit respect to the power introduced, modified by adding a parallel capacitor at the output of each circuit.

Finally, the results obtained by modifying the Greinacher circuit are shown in Figure 37. It can be seen that the circuit impedance belongs to 120-125 ohms, which increases from the input power. The behaviour that describes the circuit in high frequency is identical to the obtained in Figure 28, it does not achieve to quadruple the input voltage.

Hence, it can be proved that the addition of the 0.1 μ F capacitor is not enough to make a difference in the functionality of this circuit. This is due to self-resonance of the capacitor, which is way below the desired frequency (see annex 10.3).[13]

7 IMPLEMENTATION IN THE RF HARVESTING

This section explains the procedure used to monitor the circuits using the commercial antenna (see annex 10.3) [14] as the power supply. To monitor the amount of load accumulated by rectifying the RF input, a Source Monitoring Unit (SMU) is used, specifically the model N6705C of Keysight.

The N6705C SMU is ideal for measuring low signals (up to $50\mu\text{V}$ and 8nA), as it has an infinite input impedance, it makes floating measurements, i.e. they are independent of the ground to which the device's cover is connected [5], and these measurements can also be made at 4-wire for accurate measurements without the measuring equipment affecting the measurement itself. With this type of measurement, the leakage current that may exist when performing a two-wire measurement is compensated. In this way, high precision and high resolution measurements can be performed.

In order to prove that the harvesting system is capable of obtaining a large enough amount of load to excite the energy management state, a minimum input voltage of 330mV is required, which is enough for the low power electronics to start.

When the energy harvester has passed the cold start state only 80 mV are required at the input stage and be capable of accumulating charge in storage elements of up to 5.2 V , depending on the output and polarization of the BQ25570 device [15].

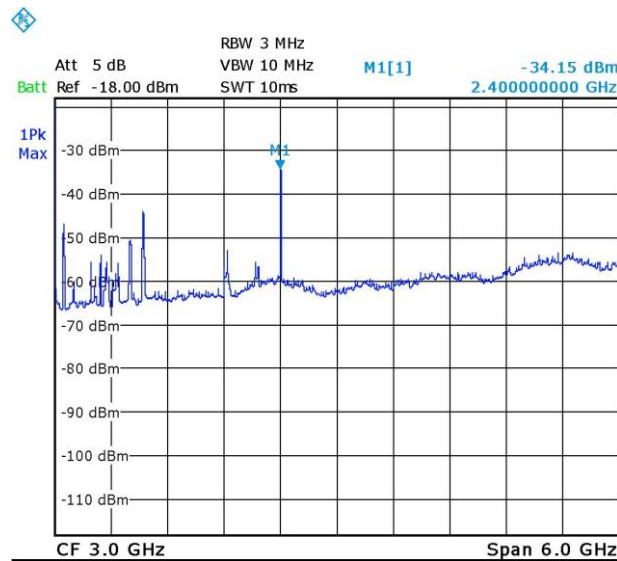


Figure 38. Frequency response of the antenna for a frequency range of 6 GHz obtained with the measurement environment described.

The test plan followed to perform the measurements requires to place the antenna approximately 4-5 meters away from the nearest router, with obstacles such as walls and others in between. The router used is a commercial model. The spectrum analyzer is used with the antenna in order to show the electromagnetic wave radiation obtained in the measurement environment, as it's shown in the Figure 38.

Taking into account all these factors, the load characterization is performed for each circuit. The circuits used correspond to those modified by adding a parallel capacity because the response obtained in the voltage doubler is favourable and does not affect the other circuits negatively.

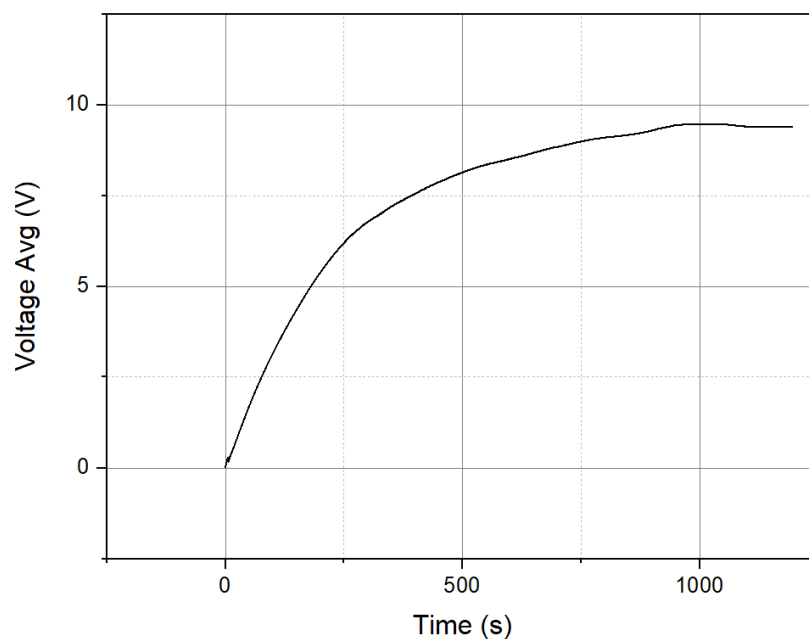


Figure 39. Monitoring of the Half wave circuit accumulated load with the antenna.

Monitoring the rectification using the Half wave rectifier, as it's shown in the Figure 39, the accumulate charge is significantly higher than the estimated value which is an inconclusive value due to working in the order of mV. In consequence, the result obtained is not decisive to comprehend the operation of this circuit.

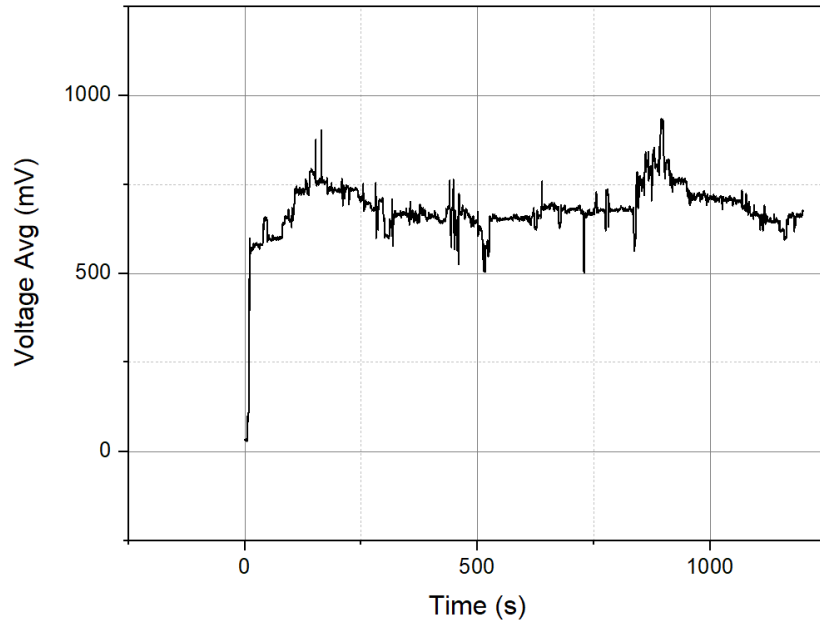


Figure 40. Monitoring of the Full wave rectifier accumulated load with the antenna.

The result obtained by rectifying with the Full wave rectifier (Figure 40) satisfies the requirements of minimum accumulated load to excite the energy management stage, which corresponds to 330 mV. An average voltage of approximately 650 mV is obtained.

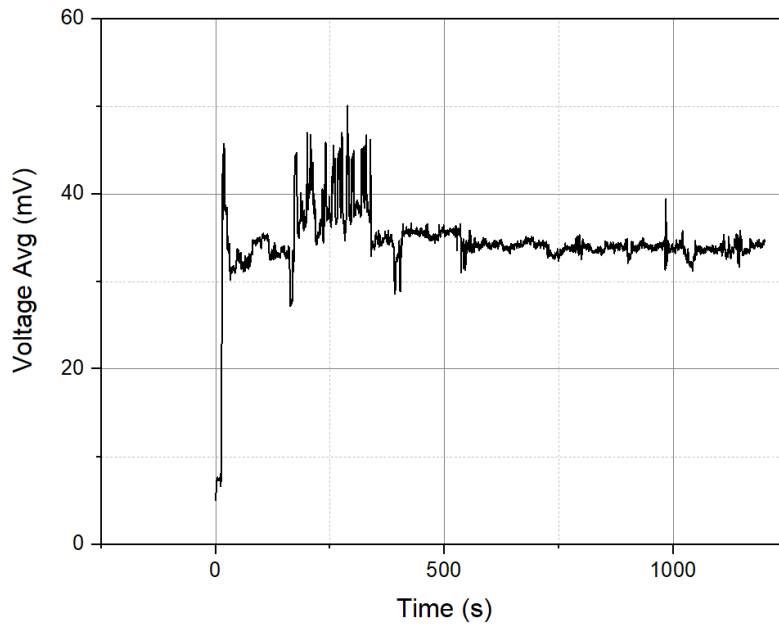


Figure 41. Monitoring of the Voltage doubler circuit accumulated load with the antenna.

The results obtained by applying the antenna to the rectifier circuit of the Figure 41 determines that this type of circuit is not capable of supplying the cold state of the harvester device, nor its subsequent state. It is determined that this circuit has not fulfilled the expectations because it requires a minimum potential to behave as a voltage duplicator, as observed in previous studies.

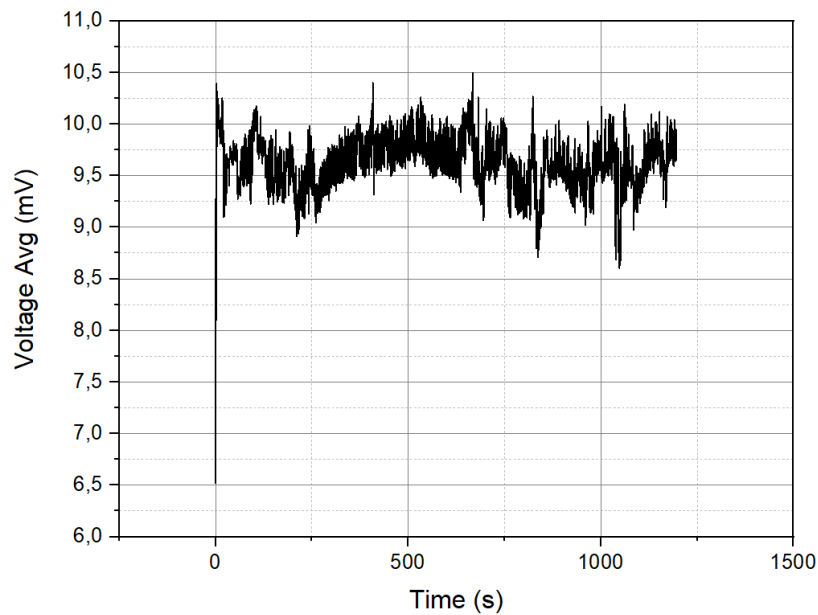


Figure 42. Monitoring of the Greinacher circuit accumulated load with the antenna.

Finally, the results obtained when applying the Greinacher circuit, are not as favourable as the voltage doubler has been observed. As mentioned above, this type of circuit requires a minimum voltage to behave as a voltage duplicator. Unlike the voltage doubler, a lower accumulated load is obtained due to the power losses due to the voltage drop across the diodes is higher.

8 CONCLUSIONS

In this work, the behaviour of half-wave rectifier, full wave rectifier and voltage multipliers has been analyzed for a wide frequency band. The study for low and high frequency is performed separately due to the complexity to monitor the results. The only way to evaluate it is observing the power level at the output of the circuits.

In chapter 4, an analysis of the different topologies is made from a circuit simulation environment where it is concluded:

- In reference to the load level, voltage multipliers are more appropriate, especially the Greinacher circuit, to obtain a high load level at the output. But to achieve this output level, requires a considerable amount of input voltage.
- On the other hand, half-wave and full wave rectifiers, in spite of obtaining an output lower than the input voltage, are able to rectify for low input voltages. Full wave rectifier obtain a more stable output than the half wave rectifier.
- As for the scalability of the circuits, a cascade configuration of the voltage doubler is achieved, while the other configurations are not feasible, due to the polarization of the diodes being affected by the addition of stages.

In chapter 5, the process of circuit assembly, measurement procedures and analyses for high and low frequency are performed.

- The results obtained in the low frequency study correspond to the simulations obtained in the previous chapter.
- The results obtained in the high frequency study shows that the voltage doubler and the full wave rectifier operates around 200 mV, meanwhile the other two circuits don't function correctly.
- Due to the full-wave rectifier operates best at low voltages, it is concluded that it is the best option for high frequency.

Due to the problems observed in the previous chapter, in chapter 6:

- The conclusion is that this is due to working with non-linear devices and within the barrier voltage of the diodes.
- As an alternative solution, the load is modified to work better at high frequency by adding a 0.1 μF . But it's not enough to make a difference in functionality, because the self-resonance of the capacitor is far below the desired frequency.

Finally, in chapter 7, the circuits are monitored as the antenna is applied, in order to see which one is able to obtain a load higher than 330 mV to power the energy management stage:

- Among all the topologies studied, the full wave rectifier has been the only capable of reaching the desired load level.
- The results obtained from the half-wave rectifier are inconclusive due to the data obtained in this chapter and in the high frequency study.
- The rectifier circuits were not implemented with the harvesting system.

From the results and conclusions extracted in the study, some aspects that could have been studied are mentioned.

From the montage of the circuits, several factors could be improved, like the realization of the circuits in PCB. The design would be optimized to suppress the losses originated by the design, such as the parasitic capacities originated by the thickness of the tracks and the proximity of them.

Because the entire spectrum must be considered when rectifying a signal, it is operated in a wide frequency band in order to take advantage of the power of the spectrum. For this reason, no impedance matching is required for a specific frequency. As a result, losses occur in the rectification of circuits, which among other things can affect their operation. On the other hand, it should be studied whether the losses are negligible compared to the accumulated power.

9 REFERENCES

- [1] Véronique Kuhn – Cyril Lahuec – Fabrice Seguin – Christian Person, “A Multi-Band Stacked RF Energy Harvester with RF-to-DC Efficiency Up to 84%”, IEEE Transactions on microwave theory and techniques, May 2015.
- [2] Elsevier, “Scopus. Abstract and citation database of peer-reviewed literature: scientific journals, books and conference proceedings”, Database, 2020, [Online]: <https://www.scopus.com/search/form.uri?display=basic>
- [3] CATRENE Scientific Committee, “Energy Autonomous Systems: Future trend in devices, technology, and systems”, CATRENE Working Group on Energy Autonomous Systems, 2009.
- [4] Simon Hemour – Ke Wu, “Radio-frequency rectifier for electromagnetic energy harvesting: Development path and future outlook”, Proceedings of the IEEE, 2014.
- [5] Martínez de Arriba, Guillem, “Diseño de un sistema de Energy Harvesting para RF”, Electronic Engineering of Telecommunications, Universitat Autònoma de Barcelona, June 2018.
- [6] Guillem Martínez – Ertugrul Coskuner – Joan J. García, “Enhanced RF harvesting system by the utilization of resonant cavities”, PATMOS 2018.
- [7] A.P. Godse – U.A. Bakshi, “Electronic Devices And Circuits”, Technical Publications Pune, 2009.
- [8] Farnell, “Datasheet RF Schottky Diode Single”[Online]. Available: 4/12/2019. http://www.farnell.com/datasheets/1697931.pdf?_ga=2.164466047.1348634823.1575801084-725668482.1575801084
- [9] Aspencore, “Voltage multiplier circuit”, Blog, 2020, [Online]: <https://www.electronics-tutorials.ws/blog/voltage-multiplier-circuit.html>
- [10] Farnell, “Datasheet SMD Multilayer Ceramic Capacitor, 4.7 μ F”[Online]. Available: 4/12/2019. http://www.farnell.com/datasheets/2741388.pdf?_ga=2.168742625.1348634823.1575801084-725668482.1575801084
- [11] TDK Corporation, “Ceramic capacitors”, Article, 2019, [Online]: https://www.tdk.com/tech-mag/electronics_primer/6

- [12] Norbert R. Malik, “ Circuitos electrónicos: análisis, simulación y diseño”, Prentice Hall, 1998.
- [13] Farnell, “ Datasheet SMD Multilayer Ceramic Capacitor, 100000 pF” [Online]. Available: 15/01/2020.
http://www.farnell.com/datasheets/2237835.pdf?_ga=2.161934524.1422455161.1579682493-725668482.1575801084
- [14] Molex, “Datasheet 2.4 GHz/5GHz Wi-Fi stand alone antenna compatible with U.FL/I-PEX MHF connectors” [Online]. Available: 15/01/2020.
https://www.molex.com/molex/products/datasheet.jsp?part=active/0479500011_AN_TENNAS.xml
- [15] Texas Instrument, “ Datasheet BQ25570 nano power boost charger and buck converter for energy harvester powered applications” [Online]. Available: 28/12/2019.
<https://www.ti.com/lit/ds/symlink/bq25570.pdf>

10 ANNEX

10.1 ANNEX 1 - PAPER PATMOS 2018 [6]

Enhanced RF harvesting system by the utilization of resonant cavities

Guillem Martínez de Arriba
Grupo de Aplicaciones
ElectroMagneticas Industriales (GAEMI)
Dept. Enginyeria Electronica)
Universitat Autònoma de Barcelona
Cerdanyola del Vallès, Spain
guillem20121995@gmail.com

Ertugrul Coskuner
Grupo de Aplicaciones
ElectroMagneticas Industriales (GAEMI)
Dept. Enginyeria Electronica)
Universitat Autònoma de Barcelona
Cerdanyola del Vallès, Spain
ertugrul.coskuner@e-campus.uab.cat

Joan J. Garcia-Garcia
Grupo de Aplicaciones
ElectroMagneticas Industriales (GAEMI)
Dept. Enginyeria Electronica)
Universitat Autònoma de Barcelona
Cerdanyola del Vallès, Spain
joan.garcia@uab.es

Abstract—This paper proposes a novel approach to the problem of harvesting the energy of the RF spectrum. Unlike the unusual impedance matching network, the combination of a Fabry-Perot cavity with commercial Wi-Fi antennas is proposed to enhance the energy capture in frequency range between hundreds of MHz and few GHz energy of a wide band. To show the viability of the method, an illustrative prototype has been implemented and tested. The experimental measurements shows the viability of the approach. Work is in progress to combine the enhanced RF transducer with standard energy management in order to test the efficiency of a full harvesting system with load capacity up to 5.2 V.

Keywords—RF, harvesting, antenna, energy management.

I. INTRODUCTION

The imminent deployment of the IoT devices requires more and more efficient low power sources. Numerous approaches to the old idea of Electro-Magnetic radiation harvesting system [1, 2] are emerging recently focused in the RF range and more specifically focused in the Wi-Fi frequencies [3, 4, 5, 6]. However, there is still a long way to develop a clear scheme for a full and reliable RF harvesting system. Many of the more popular approaches uses concepts and tools inherited from the telecommunication signal field that can be not only not appropriate but even counterproductive. The rectification of electromagnetic waves caught by the antenna is done usually using Schottky diodes in a high non-linear rectifier stage. This high non-linearity behaviour puts into question the utilization of impedance matching networks since the power will be dispersed into multiple frequency components.

This work proposes a wideband alternative to the impedance matching networks able to collect energy from the main communication frequency bands up to 5 GHz. The basic idea is to combine an antenna with a resonant cavity, in such a way that the reflection wave, if any, can be recollected and confined by the cavity and re-captured by the antenna in what we call enhancement energy transducer process. As an illustrative example, the effects of a normal antenna and the enhanced system over a very basic harvesting system are compared. The RF rectifier is formed by a four Schottky diodes in a full bridge rectifier configuration connected to an 8 mF supercapacitor acting as storage element. The improved RF transducer has proven capable of doubling the energy uptake capacity compared to single antenna RF.

II. ABOUT THE IMPEDANCE MATCHING IN RF HARVESTING SYSTEMS.

Many RF harvesting systems include a matching network [2]. In theory, this impedance matching stages avoid power reflections; however, the technique is applicable only in linear systems and usually only works for a single frequency. In our opinion, these networks are structures very useful in the field of communications but they become a drawback when approaching the problem of rectifying RF waves. This work proposes a completely different approach to extract energy from the electromagnetic spectrum in the RF range.

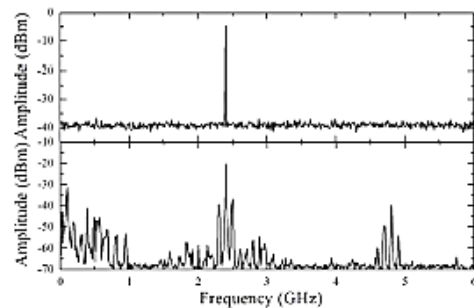


Fig. 1. Measured spectrum of: (a) single mode excitation at 2.4 GHz (b) spectrum of the single mode after four diodes bridge rectification stage indicating the power frequency dispersion in the rectification process.

The diodes are the main milestone of the RF rectification problem [1]. To be useful and efficient at such frequencies these devices have to be able to operate with high frequency signals and exhibit a low forward biased voltage. The more common choice is the Schottky diodes which can easily operate at the GHz range with typical forward voltage between 150 and 450 mV. In any case, diodes are highly non-linear devices, especially when operating in the conduction limits.

The typical rectification RF circuit uses 4 of these highly non-linear devices in a bridge configuration (see figure 2), since the objective of the rectification process is to transform sinusoidal waves in all-positive waves. The fact that the input wave has to be transformed in an only-positive-voltage-wave, points out the question of at which frequency the impedance

matching should be done. Fig. 1 shows the frequency spectrum of a monochromatic pulse centred at 2.4 GHz before and after the rectification, becoming evident the high dispersion of the resulting wave with components before 1 GHz, and around 2.4 and 5 GHz.

As result of this frequency power dispersion, the application of a traditional network matching technique, based on a single resonant frequency, will results highly inefficient since although the matching stage will optimise the power transfer at the resonant frequency, it also acts as a filter for the rest of the spectrum with the consequent lost in power performance.

To overcome this situation, and with the aim to optimize the RF energy harvest, a completely different approach without the impedance matching network is proposed in this work.

III. THE PROPOSED ENHANCED RF TRANSDUCTOR.

It is well known that, the RF cavities can storage energy and have been widely used microwave engineering [7]. Our approach takes advantage of the fact that the electromagnetic waves are reflected by metallic walls making possible to confine the RF power in the region of the antenna enhancing the possibility to re-catch the reflected energy. Since the microwave reflection phenomena is independent of the frequency, it is expected that the confinement effect is not restricted to a particular frequency obtaining a wideband energy re-caught effect. It is clear that in such a system the signal coherence will be destroyed by multiple interferences but it is not necessary since our interest is focused in the power of the signal and not in the information they carry.

With the aim to illustrate the concept, a simple prototype has been implemented in which the antenna is located and grounded into the cavity as can be seen in the Fig. 2.

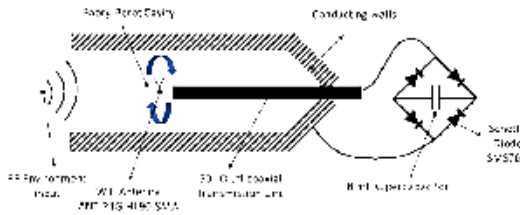


Fig. 2. Scheme of the antenna between the two Fabry-Perot metallic layers.

The open space in the cavity allows the antenna to receive the ambient RF signal. The antenna is connected to a 50 Ohms transmission line which lead to the rectifier and storage elements which is formed by a 4 Schottky diodes bridge supplying charge to a 8 mF supercapacitor. Since the system is non-matched and highly nonlinear, it is expected that some of the incoming power will be reflected and, eventually emitted by the antenna inside the Fabry-Perot cavity. Fig. 3 shows the spectrum caught by the antenna up 6 GHz, in which we would like to focus our harvesting enhanced transductor.

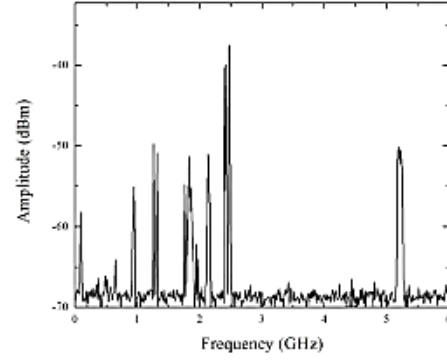


Fig. 3 Measured spectrum of the commercial antenna used in the implementation of the enhanced RF transductor prototype.

At this point, the EM energy confinement into the cavity will propitiate that some of the RF reflected energy will be re-caught by the antenna in an iterative course. It is expected that this process improves the energy caption capability of the whole harvesting system by two different ways. First of all, there is the fact that the energy capture is not limited to a single frequency. In the matched harvesting systems, the impedance matching use to be optimum only for a single frequency and the matching networks attenuate the power incoming from the rest of the spectrum.

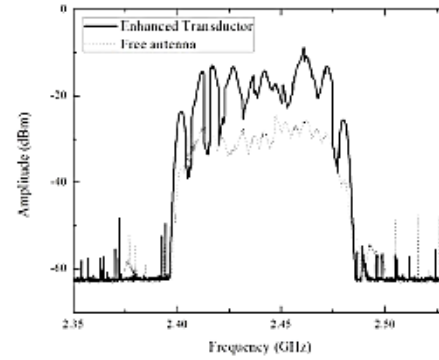


Fig. 4. Differences in Maximum power captured in the wi-fi frequency range corresponding with the IEEE 802.11 standard.

This broadband behaviour of the proposed harvesting system, shown in Fig. 2, allows to extract energy from all the spectrum visible by the antenna (see Fig. 3) and not from a single frequency as usual. On the other hand, the Fabry-Perot cavity increases the energy caption capability of the antenna (in the full bandwidth). It may be not as much effective such as an impedance matching for a single frequency, but the wide band nature and the energy re-appropriation issued by the Fabry-Perot cavity compensate the mismatch drawbacks.

Fig. 4 shows the comparison between the power recollectd by the free antenna in with the collected by the enhanced RF transductor around the 2.4GHz Wi-Fi channels. An average improvement of 10 dBm can be observed in the case of the proposed system in the figure 2.

The power increment observed in Fig. 4 in the proposed transductor is similar in all the antenna spectrum. Therefore, the final collected energy will result of the contribution of by the antenna, in such a way that the possible losses due to the mismatch are widely compensated by the ability to collect energy in the antenna operating frequency range.

The performance of the proposed system described in figure 2, can be observed in Fig. 5 in comparison with the free antenna. In both cases the storage element is 8 mF supercapacitor. How measurements are made is a matter to be in mind. The input impedance of the measuring device can disturb the results. With the goal of improving the measurements accuracy, a 4-wire set up has been established using an DC Power Analyzer (N6705C with two N6781A modules). As can be observed the enhanced system is able to achieve a solid average value of 400 mV while the single antenna just arrives to an average value of 200 mV. Since the minimal voltage required by the energy management integrated circuit (for instance the BQ2570 from Texas Instrument) use to be typically around 300 mV, according with the results showed in figure 6, the proposed enhanced RF transductor formed by the antenna and the Fabry-Perot cavity, makes viable a full RF harvesting system able to charge batteries up to 5.2 V.

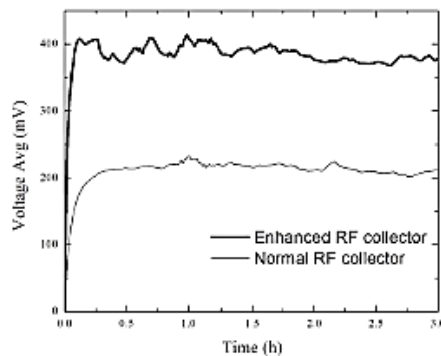


Fig. 5. Performance comparison between the free antenna and the proposed enhanced transductor, using an N6705C DC power analyzer.

Work is in progress to evaluate the efficiency of the full RF harvesting system in different significant systems. At the moment, it has been possible to charge 1.8 V in a 120 mF supercapacitor in 17 hours or 22 mF in 7 hours achieving the same voltage.

IV. CONCLUSIONS

In this work, with the aim to use all the spectrum and not only a single resonant frequency, an alternative solution to the impedance matching has been proposed and tested. By the combination of a Fabry-Perot cavity with a conventional Wi-fi antenna an efficient RF energy transductor has been fabricated. The prototype of the enhanced RF energy harvesting system has demonstrated a 100% performance increment in comparison with a commercial free Wi-Fi antenna. The proposed RF transductor has demonstrated its viability to storage enough charge and energy to activate and supply standard electronic management stage. Work is in progress to improve the efficiency of the system by the combination of several antennas.

REFERENCES

- [1] Simon Hemour, and Ka Wu, Radio-Frequency Rectifier for Electromagnetic Energy Harvesting: Development Path and Future Outlook, *Proceedings of the IEEE*, Vol. 102, No. 11, November 2014.
- [2] Le-Giang Tran, Hyoun-Kyu Cha and Woo-Tae Park1, "RF power harvesting: a review on designing methodologies and applications", Tran et al. *Micro and Nano Syst Lett* (2017).
- [3] Morteza Biglari-Abbasi and Kean C. Aw, "Indoor 2.45 GHz Wi-Fi Energy Harvester with Bridgeless Converter", *IEEE journal on selected areas in communications*, May 2016.
- [4] Pouya Kamalinejad et al., "Wireless Energy Harvesting for the Internet of Things (IoT)", *IEEE Communications Magazine*, June 2015
- [5] Allen M. Hawkes, Alexander R. Katko and Steven A. Cummer, "A microwave metamaterial with integrated power harvesting functionality, AIP publishing, 2013.
- [6] Ugur Olgun, Chi-chih Chen, and John L. Volakis, "Efficient Ambient Wi-Fi Energy Harvesting Technology and its applications", *IEEE*, 2012.
- [7] R. N. Clarke and C. B. Rosenberg, "Fabry-Perot and open resonators at microwave and millimeter wave frequencies, 2-300 GHz", *J. Phys. E: Sci. Instrum.* 15 9, pp. 9-24, 1982.

10.2 ANNEX 2 - DATASHEET OF THE SCHOTTKY DIODE SMS7630 [8]

Parameter	Units	SMS1546 Series	SMS7621 Series	SMS7630 Series
Is	A	3E-7	4E-8	5E-6
Rs	Ω	4	12	20
N	–	1.04	1.05	1.05
Tt	sec	1E-11	1E-11	1E-11
Cj0	pF	0.38	0.1	0.14
M	–	0.36	0.35	0.40
Eg	eV	0.69	0.69	0.69
Xti	–	2	2	2
Fc	–	0.5	0.5	0.5
Bv	V	3	3	2
Ibv	A	1E-5	1E-5	1E-4
Vj	V	0.51	0.51	0.34

Figure 43. Spice parameters of the Schottky diode SMS7630.

a)

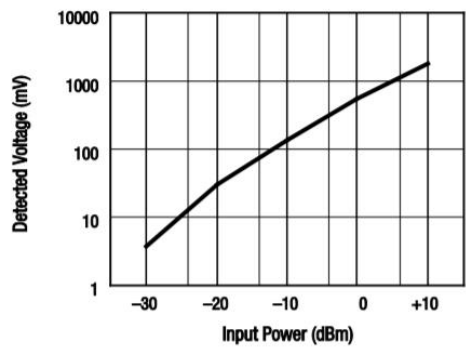


Figure 3. Typical Detector Characteristics @ 1.8 GHz

b)

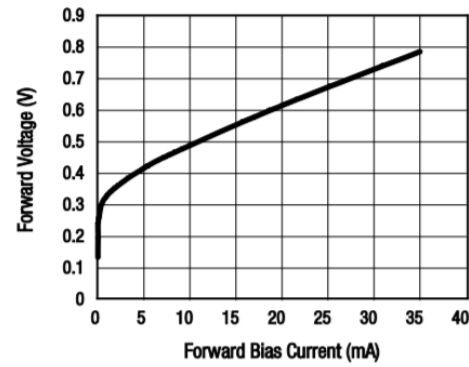


Figure 4. SMS7621-081LF Forward Voltage vs Forward Bias Current

Figure 44. a) Typical detector characteristics at 1.8 GHz and b) Forward voltage vs forward bias current for the Schottky diode.

10.3 ANNEX 3 - DATASHEET OF THE SMD CERAMIC CAPACITOR OF 0.1 μ F [13]

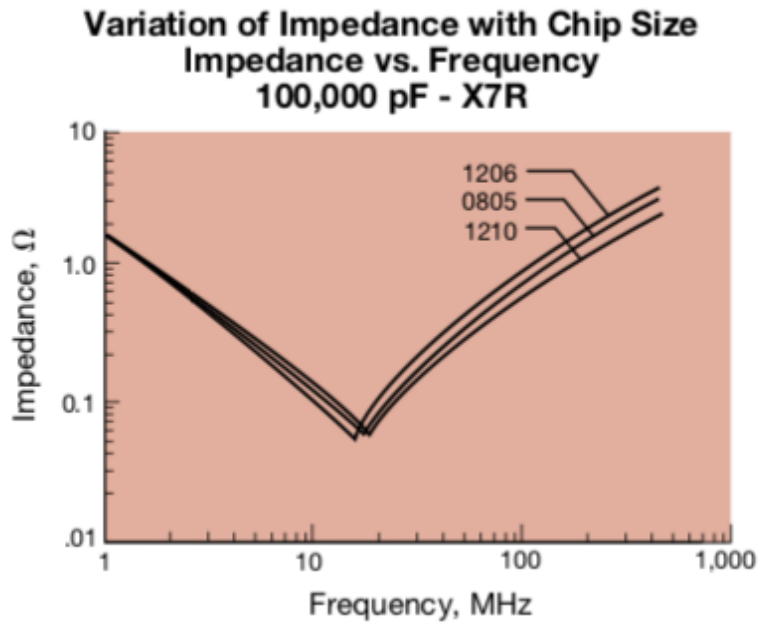


Figure 45. Variation of impedance with chip size vs frequency for 0,1 μ F.

10.4 ANNEX 4 - DATASHEET OF THE 2.4 GHz/ 5 GHz WI-FI ANTENNA[14]

Band#1 F_End (MHz)	2483.5
Band#1 F_Start (MHz)	2400
Band#2 F_End (MHz)	5900
Band#2 F_Start (MHz)	4800
Electrical Connectivity	Cable
Peak Gain (dBi)	2.27 @ 2.4 GHz, 4.9 @ 5 GHz
Return Loss - S11 (dB)	< -10, < -9
Total Efficiency	>85% @ 2.4 GHz, >85% @ 5 GHz

Figure 46. Electric specifications of the Wi-Fi antenna.

Resum:

Aquest projecte tracta d'analitzar i caracteritzar la quantitat d'energia recol·lectada provinent d'una àmplia banda de freqüències per tal d'excitar una etapa electrònica de gestió d'energia. L'estudi explora les diferents tipologies de circuits rectificadors per obtenir la conversió de ràdio freqüència a corrent continu més òptima.

Resumen:

Este proyecto trata de analizar y caracterizar la cantidad energía recolectada proveniente de una amplia banda de frecuencias con el fin de excitar una etapa electrónica de gestión de energía. El estudio explora las diferentes topologías de circuitos rectificadores para obtener la conversión de radio frecuencia a corriente continua más óptima.

Summary:

This project aims to analyze and characterize the amount of energy collected from a wide band of frequencies in order to excite an electronic stage of energy management. The study explores the different rectifier circuit topologies to achieve the most optimal radio frequency to direct current conversion.